iScience

CellPress
OPEN ACCESS

Article

Superoxide dismutase gene family in cassava revealed their involvement in environmental stress via genome-wide analysis

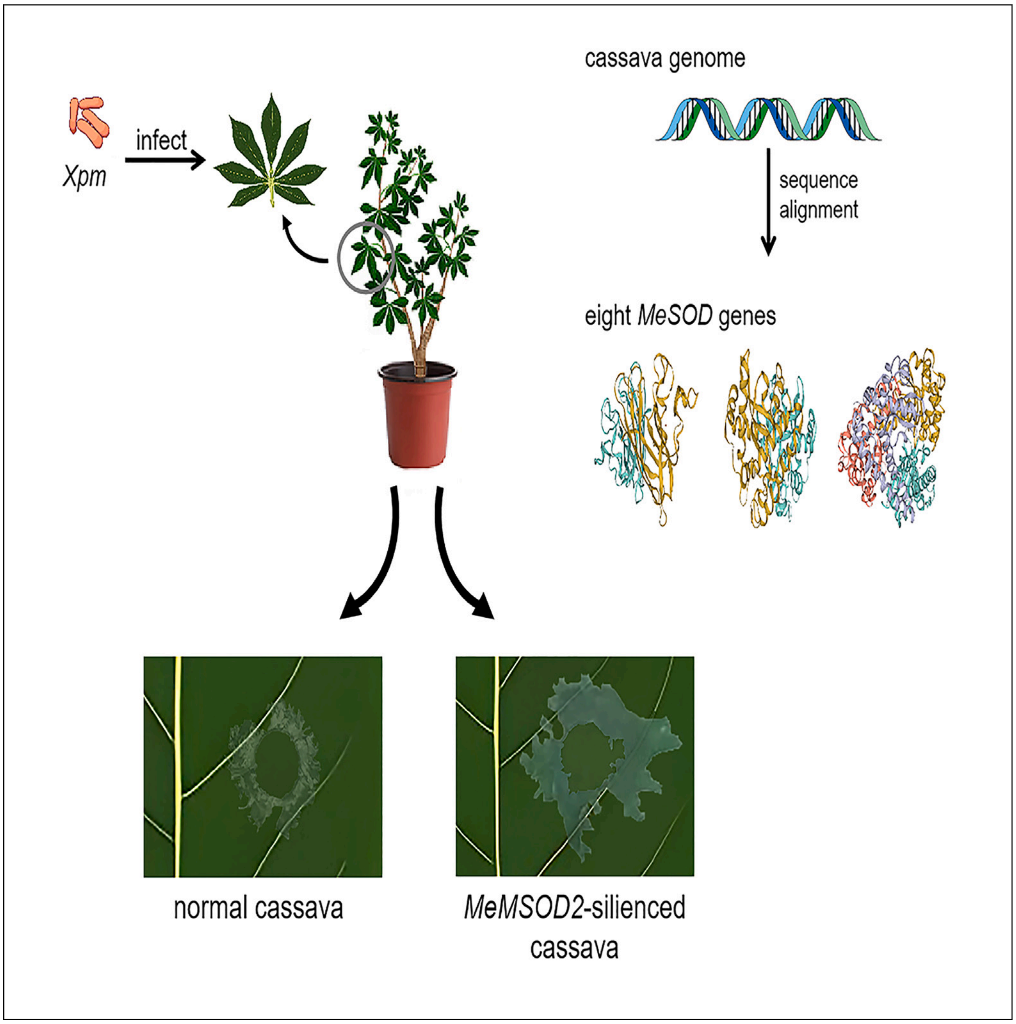

Linling Zheng, Abdoulaye Assane Hamidou, Xuerui Zhao, ..., Xiaofei Zhang, Kai Luo, Yinhua Chen

luok@hainanu.edu.cn (K.L.)
yhchen@hainanu.edu.cn (Y.C.)

Highlights

4 CSODs, 2 FSODs, and 2 MSODs gene families were identified within the cassava genome

MeCSOD2 was induced by salt stress

MeMSOD2 responded to drought and cassava bacterial blight stresses

MeMSOD2 gene silencing increased *Xpm*CHN11 virulence

Zheng et al., iScience *26*, 107801
October 20, 2023
https://doi.org/10.1016/j.isci.2023.107801

iScience

Article

Superoxide dismutase gene family in cassava revealed their involvement in environmental stress via genome-wide analysis

Linling Zheng,[1,5] Abdoulaye Assane Hamidou,[1,5] Xuerui Zhao,[1] Zhiwei Ouyang,[2] Hongxin Lin,[3] Junyi Li,[1] Xiaofei Zhang,[4] Kai Luo,[1,*] and Yinhua Chen[1,6,*]

SUMMARY

Superoxide dismutase (SOD) is a crucial metal-containing enzyme that plays a vital role in catalyzing the dismutation of superoxide anions, converting them into molecular oxygen and hydrogen peroxide, essential for enhancing plant stress tolerance. We identified 8 SOD genes (4 CSODs, 2 FSODs, and 2 MSODs) in cassava. Bioinformatics analyses provided insights into chromosomal location, phylogenetic relationships, gene structure, conserved motifs, and gene ontology annotations. *MeSOD* genes were classified into two groups through phylogenetic analysis, revealing evolutionary connections. Promoters of these genes harbored stress-related *cis*-elements. Duplication analysis indicated the functional significance of MeCSOD2/MeCSOD4 and MeMSOD1/MeMSOD2. Through qRT-PCR, MeCSOD2 responded to salt stress, MeMSOD2 to drought, and cassava bacterial blight. Silencing MeMSOD2 increased *Xpm*CHN11 virulence, indicating MeMSOD2 is essential for cassava's defense against *Xpm*CHN11 infection. These findings enhance our understanding of the SOD gene family's role in cassava and contribute to strategies for stress tolerance improvement.

INTRODUCTION

In the face of diverse biotic and abiotic stresses, crop productivity is often hampered, posing a significant threat to global food security. As sessile organisms, plants have evolved intricate defense mechanisms to respond effectively to environmental cues.[1] One such challenge arises from reactive oxygen species (ROS). Cellular metabolism generates ROS that results in damage to biological macromolecules, biofilms, and other structures; leading to cell death in severe cases, including superoxide anion radicals (O_2^-), hydrogen peroxide (H_2O_2), hydroxyl radicals (OH^-), peroxyl radicals (HOO^-), and singlet oxygen ($^1O_2$).[2–4] Aerobic organisms have developed antioxidative defense mechanisms to deal with ROS. There are a few types of antioxidant enzymes within the biological system, and the most common that play important roles in scavenging free radicals are superoxide dismutase (SOD), catalase (CAT), peroxidase (POD), and glutathione peroxidase (GPx).[5–8] SODs are the first line of defense against ROS within cell.[9] Therefore, increased SOD expression can protect plants against environmental stresses. For instance, Overexpression of the *Arabidopsis* and winter squash SOD genes improves chilling tolerance in transgenic *Arabidopsis* via ABA-sensitive transcriptional regulation.[10]

SODs catalyze the conversion of superoxide radicals (O_2^-) into hydrogen peroxide (H_2O_2), which is then further converted to non-toxic water (H_2O) and oxygen (O_2).[11] SODs are classified into four groups based on the metal cofactors found in their active sites, including copper-zinc SOD (Cu/Zn-SOD), manganese SOD (Mn-SOD), iron SOD (Fe-SOD), and nickel SOD (Ni-SOD).[12,13] Cu/Zn-SOD is predominantly found in higher plants, whereas Mn-SOD and Fe-SOD are predominantly found in lower plants.[14] Ni-SOD is mainly found in cyanobacteria, *Streptomyces,* and marine life.[15,16] These SODs are unequally distributed throughout all biological kingdoms and in various cell compartments.[9] Cu/Zn-SOD is mainly detected in the mitochondria, chloroplast, and cytosol, whereas Mn-SOD is mainly detected in the mitochondria and peroxisomes. In contrast, Fe-SOD is mainly detected in mitochondria, chloroplasts, and peroxisomes.[17] A comparison of deduced amino acid sequences from Mn-SOD, Fe-SOD, and Cu/Zn-SODs suggests that Mn-SOD and Fe-SOD are more ancient SODs. These enzymes most likely evolved from the same ancestral enzyme. In contrast, Cu/Zn-SODs showed no sequence similarity to Mn-SOD and Fe-SODs and probably evolved separately in eukaryotes.[18,19] Interestingly, Cassava's combined expression of Cu/Zn-SOD and CAT improves tolerance to cold and drought stresses.[20]

[1]Sanya Nanfan Research Institute of Hainan University, School of Life Sciences, Hainan University, Sanya 572025, China
[2]HNU-ASU Joint International Tourism College, Hainan University, Haikou 570228, China
[3]Soil Fertilizer and Resources Environment Institute, Jiangxi Academy of Agricultural Sciences, Nanchang 330200, China
[4]Alliance of Bioversity International and the International Center for Tropical Agriculture (CIAT), Cali 763537, Colombia
[5]These authors contributed equally
[6]Lead contact
*Correspondence: luok@hainanu.edu.cn (K.L.), ychen@hainanu.edu.cn (Y.C.)
https://doi.org/10.1016/j.isci.2023.107801

Table 1. SOD genes identified from *M. esculenta* and their sequence information

Gene Name	Locus ID	Chromosome Location	CDS Length (bp)	AA[a]	MW[b] (Da)	pI[c]	GRAVY[d]	Sublocation (WoLF)
MeCSOD1	Manes.02G028800.1	Chr02:2215898:2219178	978	326	34620.32	5.91	−0.090	chloroplast
MeCSOD2	Manes.08G125400.1	Chr08:29047236:29051036	459	153	15114.69	5.42	−0.143	cytoplasm
MeCSOD3	Manes.08G145300.1	Chr08:31046344:31049768	480	160	16081.07	6.58	−0.176	cytoplasm
MeCSOD4	Manes.09G160400.1	Chr09:27490633:27493759	459	153	15310.95	5.85	−0.169	cytoplasm
MeFSOD1	Manes.04G064500.1	Chr04:17777222:17782573	837	279	32142.95	7.08	−0.381	chloroplast
MeFSOD2	Manes.06G129100.1	Chr06:23592592:23595228	819	273	30622.72	6.66	−0.427	mitochondria
MeMSOD1	Manes.07G140500.1	Chr07:26513248:26516765	702	234	25864.52	7.82	−0.337	mitochondria
MeMSOD2	Manes.10G000300.1	Chr10:8619:15017	708	236	26179.91	8.62	−0.241	mitochondria

[a]Length of amino acid sequence.
[b]Molecular weight of the amino acid sequence.
[c]Isoelectric point of the *MeSOD*.
[d]Grand average of hydropathicity.

SOD gene family has been reported in various plants, including *Arabidopsis thaliana*,[21] *Musa acuminata*,[22] *Lycopersicon esculentum*,[23] *Gossypium*,[24] *Cucumis sativus*,[25] *Dimocarpus longan*,[26] *Setaria italica*,[27] *Vitis vinifera*,[28] *Triticum aestivum*,[29] and *Brassica juncea*.[30] Previous studies revealed that SOD could protect plants against biotic and abiotic stresses.[31] For example, the anti-cytosolic FSOD (cyt-FSOD) contents were upregulated dramatically in soybean tissues under stress conditions such as drought or nitrate excess.[32] The transgenic *A. thaliana* and *Triticum turgidum* L. subsp. *Durum* Mn-SOD (*TdMnSOD*) exhibited high tolerance to salt and drought stresses.[33] Moreover, when the transgenic cassava lines over-producing Cu-ZnSOD were tested against the spider mite *Tetranychus cinnabarinus*, they showed less damage than the wild type.[34]

Cassava (2n = 36, *Manihot esculenta* Crantz) is a staple food crop in the tropics and sub-tropics, cultivated as a subsistence crop. It was likely the first domesticated species over 10,000 years ago.[35,36] Cassava is the main source of dietary calories for more than 800 million people worldwide (Fao, 2013). In addition, cassava is used for bioenergy storage to produce high starch products with minimal processing costs due to its high starch accumulation in its tuber roots.[37,38] Compared to most major food crops, cassava yield remains relatively stable under various environmental stresses, particularly drought and low fertilisation.[36,39] Nevertheless, the mechanisms underlying cassava resistance to abiotic stress remain largely unexplored.[40] Cassava's most serious bacterial disease is Cassava Bacterial Blight (CBB), caused by *Xanthomonas phaseoli* pv. *Manihotis* (*Xpm*).[41] CBB threatens food security in tropical regions and can generate up to 100% losses under unfavorable climatic conditions (CABI, 2015; FAO, 2008).[42] The rapid spread of CBB in some cassava-producing regions highlights the necessity of developing novel methods to control this disease.[43–46] The release of the cassava genome lays the groundwork for genome-wide analysis of new gene resources,[47] which may provide effective ways to improve stress tolerance in cassava genetically. Nonetheless, studies on the molecular mechanisms of CBB resistance are scarce.[48] The characteristics underlying the biotic stress response of cassava remain largely unexplored. Many genes, such as SOD, have yet to be identified in cassava.[49]

Hence, this study aimed to characterize the SOD gene family in the cassava genome. Eight SOD genes were identified and unevenly distributed on seven chromosomes, and characteristics including physicochemical properties, evolutionary relationships, structural characteristics, synteny analysis, promoter *cis*-elements, and GO annotation were investigated. In addition, the expression profiles of SOD genes in response to drought, salt, and biotic (CBB) stress were investigated using quantitative real-time PCR (qRT-PCR). In addition, Our findings demonstrated that silencing MeMSOD2 increases the virulence of cassava bacterial blight (*Xpm*CHN11), as confirmed by Real-Time Quantitative Reverse Transcription PCR (qRT-PCR) and Virus-induced gene silencing (VIGS) techniques. Therefore, MeMSOD2 is essential for cassava's defense against *Xpm* infection. This study provides comprehensive insights into SOD genes in cassava and sheds light on their possible functions in environmental stress tolerance.

RESULTS

Eight SOD gene family members were identified in the cassava genome

Eight conserved SOD homologs in cassava's reference genome were identified after rigorous bioinformatic analyses, including 4 CSODs, 2 FSODs, and 2 MSODs (Table 1). The predicted protein length of *MeSOD* genes ranged from 153 (*MeCSOD2*) to 326 aa (MeCSOD1), with the molecular weight (MW) varying from 15.11 (MeCSOD2) to 34.62 kDa (MeCSOD1), and the CDS length from 459 (MeCSOD2) to 978 bp (MeCSOD1). *MeSOD* genes had a negative GRAVY, indicating they were all hydrophilic.[50] Subcellular localization prediction revealed that MeMSODs were localized in mitochondria, MeCSODs predominantly in cytoplasm and chloroplast, and MeFSODs in chloroplast and mitochondria (Table 1).

The conserved domains in *MeSOD* proteins were examined using the Pfam server, and four putative conserved domains were identified, namely the sod_Cu, sod_ Fe_N, sod_Fe_C, and HMA domains (Figure 1). These putative conserved domains existed in multiple MeSOD protein sequences. Most MeSODs classified into the same clade had the same conserved domain. For example, MeFSODs and MeMSODs

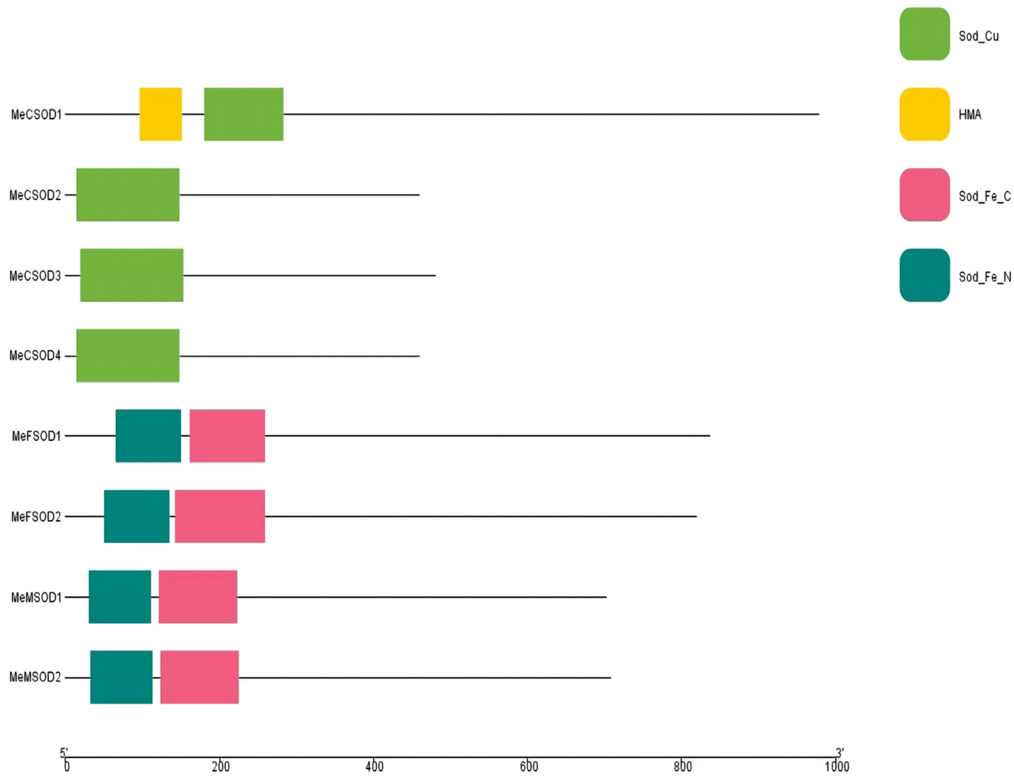

Figure 1. Conserved domain of the predicted MeSOD proteins

The conserved domains of *MeSOD* genes were predicted using the Pfam server (http://pfam-legacy.xfam.org/) and visualized with TBtools. The green, yellow, pink, and dark blue represent the sod_Cu, HMA, sod_ Fe_C, and sod_Fe_N domains, respectively.

contained two conservative domains, including sod_ Fe_N domain and sod_Fe_C domain. Three of four MeCSODs contained the sod_Cu domain, and MeCSOD1 contained the domains sod_Cu and HMA. The result of multiple sequence alignment showed that all MeCSOD proteins have copper/zinc binding domain (PF00080), MeFSOD and MeMSOD proteins have both N-terminal manganese/iron SOD domain (PF00081) and C-terminal manganese/iron SOD domain (PF02777), which was consistent with the multiple sequence alignment (Figure S1).

Chromosomal distribution and synteny relationship of *MeSOD* genes

Eight *MeSOD* genes were distributed on seven of the eighteen chromosomes (Me02, Me04, Me06, Me07, Me08, Me09, and Me10) (Figure 2). One *MeSOD* gene was identified in each of the above chromosomes except Me08, which harbored two *MeSOD* genes (MeCSOD2 and MeCSOD3). Gene duplication analysis showed that MeMSOD1/MeMSOD2 and MeCSOD2/MeCSOD4 were segmentally duplicated based on the chromosomal distribution of *MeSOD* genes, implying segmental duplication might be a major driving force in the evolution of the *MeSOD* gene family. Collinearity analysis revealed orthologous SOD genes among *M. esculenta* and the other four species (*A. thaliana*, *O. sativa*, *M. acuminata*, and *Populus trichocarpa*) (Figure 3). The syntenic analysis revealed eight SOD gene pairs (MeMSOD1/AtMSOD, MeMSOD1/AtCSOD2, MeMSOD2/AtCSOD2, MeCSOD2/AtCSOD1, MeCSOD3/AtCSOD3, MeCSOD4/AtCSOD1, MeFSOD2/AtFSOD1, and MeFSOD2/AtFSOD2) from *M. esculenta* and *A. thaliana*. One pair of SOD syntenic paralogs was identified between *M. esculenta* and *O. sativa* (MeCSOD1/OsCSOD4), and between *M. esculenta* and *M. acuminata* (MeMSOD2/MaMSOD1D). In contrast, eleven SOD gene pairs were identified from *P. trichocarpa* and cassava (MeCSOD1/PtCCS1, MeCSOD1/PtCCS2, MeCSOD2/PtCSOD1.1, MeCSOD2/PtCSOD1.2, MeCSOD3/PtCSOD3.1, MeCSOD3/PtCSOD3.2, MeCSOD4/PtCSOD1.1, MeCSOD4/PtCSOD1.2, MeFSOD2/PtFSOD2.1, MeMSOD1/PtMSOD1, MeMSOD2/PtMSOD1). The MeFSOD1 was not mapped to any of the four species syntenic blocks with SOD genes, indicating these chromosomes have undergone extensive rearrangements and fusions that could potentially result in selective gene loss. The K_a/K_s ratios of SOD gene pairs were determined to understand better the evolutionary constraints imposed on the SOD gene family (Table S1). The K_a/K_s ratios of all orthologous SOD gene pairs were less than 1, implying that the *MeSOD* gene family might have undergone purifying selection during evolution.

Phylogenetic relationship of *MeSOD* genes

A phylogenetic tree was generated to analyze the evolutionary relationship of the SOD gene family in cassava (Figure 4). The SOD proteins were classified into three categories based on their metal cofactor type: MSOD, CSOD, and FSOD. The results suggest that the three SOD

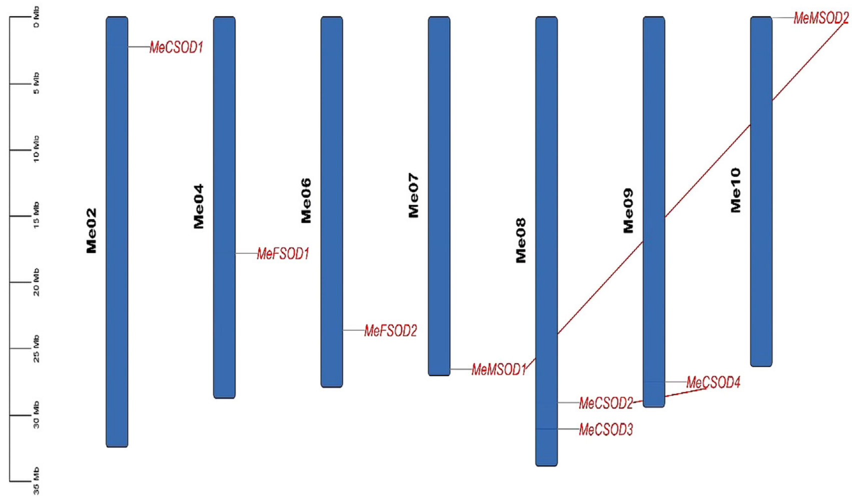

Figure 2. Chromosomal mapping of SOD genes

The chromosome numbers are indicated at the left of each chromosome. The respective genes are labeled on the left of the chromosomes. The red line connects segmentally duplicated gene pairs. Mb: megabases.

subfamilies (MSOD, CSOD, and FSOD) have a distant evolutionary relationship. The MSODs and FSODs were closely clustered, while CSODs were distinctly separated, suggesting that FSODs and MSODs might originate from a common ancestor. In addition, MeMSODs show the closest evolutionary relationship to MSODs from *P. trichocarpa* among the selected species of MSODs. However, the same *MeSOD* species, predicted to be localized in different cellular compartments, were divided into clades, such as MeFSOD1 and MeFSOD2. In addition, MeCSOD1 predicted to be localized in the cytoplasm was clustered in a different branch than those predicted to be localized in the chloroplast.

Conserved motif and exon-intron structures of *MeSOD* genes

The MEME tool predicted the conserved motifs of the *MeSOD* protein sequences. Eight putative motifs were identified. The conserved motifs of the SOD protein sequences ranged from 15 to 50 aa (motifs 5 and 4, respectively) in length and contained between two (MeCSOD1) to six (MeMSOD1 and MeMSOD2) motifs (Figure 5; Table S2). All MeCSOD protein sequences contain motifs IV and VI, indicating that these motifs are conserved in MeCSODs. In addition, all *MeSOD* protein sequences contained motif III except for MeCSOD1. The conserved motifs for F/M-SOD include motifs I, II, III, and V. The metal-binding motif "DVWEHAYY" of the MeF/M-SODs was identified in motif II (Figure 5). Motifs VII and VIII were only found in MeMSOD protein sequences. MeCSOD1 had the fewest motifs, indicating that the SOD domain may be incomplete. The *MeSOD* proteins with similar motif compositions and gene lengths may have similar functions.

Gene structure analysis (Figure 5) showed that *MeSOD* genes have a simple structure, with 5–8 introns and 6 to 9 exons. All *MeSOD* genes contained 5′ and 3′ UTRs that ranged from 37 to 1154 bp in length, except for MeMSOD2, which lacked 5′ UTRs. Most *MeSOD* genes (5) contained six exons. MeCSOD3, MeFSOD1, and MeFSOD2 contain 7, 8, and 9 exons, respectively. In contrast, MeFSOD2 had the most introns (8), while MeCSOD1, MeCSOD2, MeCSOD3, and MeMSOD1 had the fewest (5). SOD members clustered into the same clade exhibited similar exon numbers (Table S3). For instance, MeCSOD2 and MeCSOD4 had the same number of exons/introns and similar lengths. However, MeFSOD1 and MeFSOD2 contained different numbers of exons/introns.

Putative regulatory elements of *MeSOD* genes

To help characterize the gene functions and regulatory roles of *MeSOD* genes during cassava growth and stress response, potential *cis*-elements in the promoter sequences of the *MeSOD* genes were predicted using the PlantCARE database. The *cis*-elements were divided into four functional categories: light-responsive, hormone-responsive, stress-responsive, and MYB binding sites (Figure 6). Five classes of hormone-responsive *cis*-elements were identified, including abscisic acid (ABA), methyl jasmonate (MeJA), salicylic acid (SA), auxin, and gibberellin (GA), and are distributed in the promoter sequences of the *MeSOD* genes. Among these hormone-responsive *cis*-elements, ABA-responsive elements were found in the promoter sequences of MeCSOD2 and MeFSOD2, whereas auxin-responsive elements were found in those of MeCSOD3, MeMSOD1, and MeMSOD2. MeJA-responsive elements were found in four of the eight promoter sequences of *MeSOD* genes (MeCSOD1, MeCSOD2, MeCSOD3, and MeMSOD2). MeCSOD1, MeMSOD1, and MeCSOD2 promoter sequences contained GA-responsive elements, whereas MeCSOD1, MeCSOD2, and MeCSOD3 harbored SA-responsive elements. No stress-responsive elements were found in MeCSOD3 and MeFSOD2. Drought and low-temperature stress-responsive *cis*-elements were identified. Drought-responsive elements were found in MeCSOD1, MeCSOD2, MeCSOD4, MeFSOD1, and MeMSOD1, while low-temperature responsive *cis*-elements were found in MeCSOD1 and MeCSOD4. In addition, MYB binding sites were identified in other genes except MeMSOD2. Moreover, *MeSOD* genes contain numerous light-responsive elements.

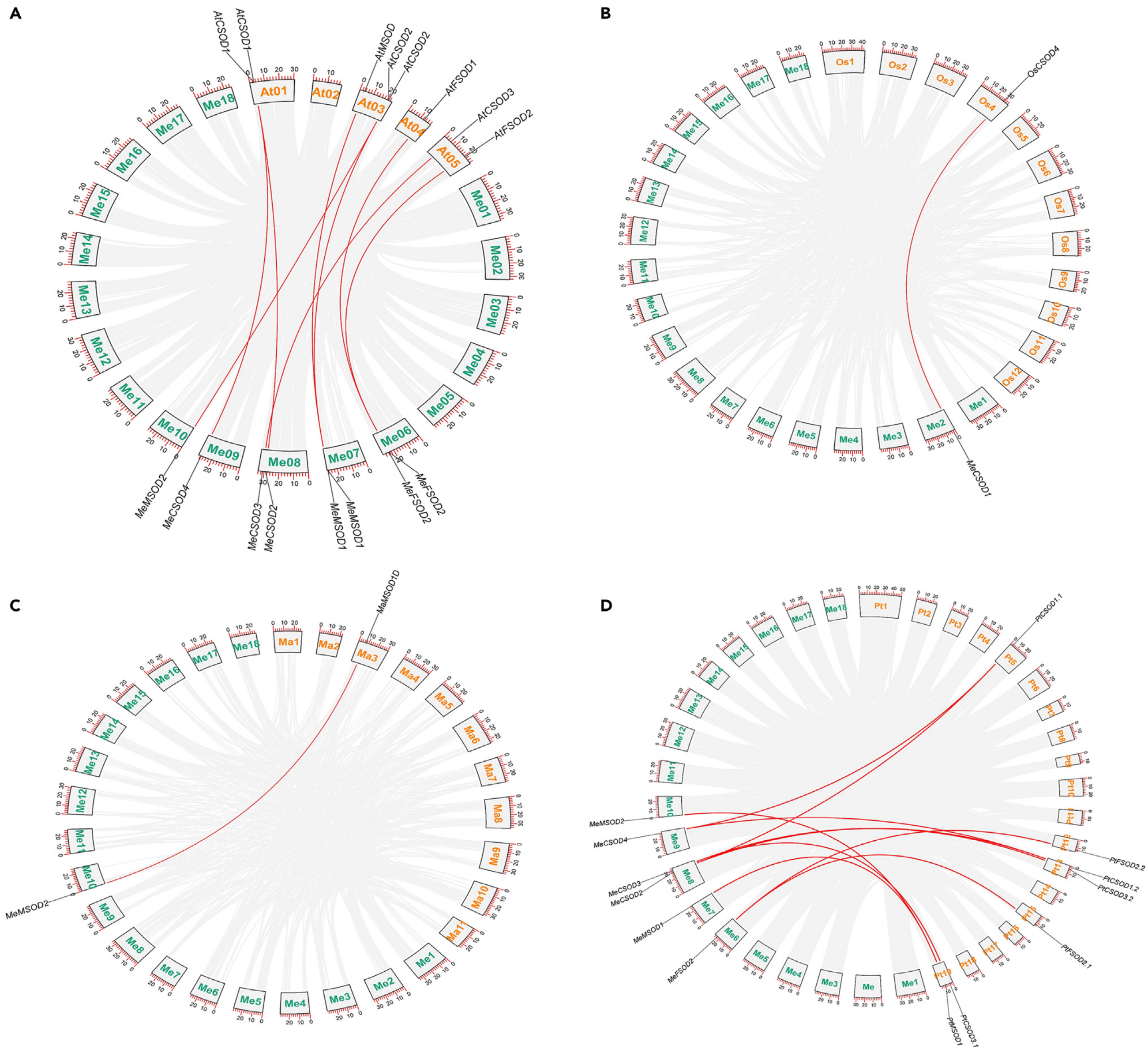

Figure 3. Synteny analysis of *SOD* genes

Synteny analysis of *SOD* genes in *A. thaliana*, *D. longan*, *O. sativa*, *M. acuminata*, *P. trichocarpa*, and *M. esculenta*. Synteny analysis of SOD genes from (A) *A. thaliana* and *M. esculenta*; (B) *O. sativa* and *M. esculenta*; (C) *M. acuminata* and *M. esculenta*; (D) *P. trichocarpa* and *M. esculenta*. Gray lines in the background indicate the collinear blocks within *M. esculenta* and the other four species. The red lines highlight the syntenic SOD gene pairs.

To investigate the miRNA-mediated post-transcriptional regulation of *MeSOD* genes, the 5′ and 3′ UTRs, and the CDS of the *MeSOD* genes were predicted for target sites of cassava miRNAs. Sixteen miRNAs from cassava targeted five *MeSOD* genes on 17 prediction sites, and all targeted sites were identified in the CDS regions (Table S4). *MeCSOD3* targeted eight miRNAs, of which seven contained continuously distributed sites. However, the miRNAs targeting *MeCSOD3* were different from the other *MeCSODs*. Besides, MeFSOD1 targeted four miRNAs with continuously distributed sites. Among the 16 miRNAs in cassava, only *mes-miR171d* targeted two *MeSOD* genes (MeCSOD2 and MeCSOD4), a pair of orthologous genes similar to the results of previous analyses.

PPI network of *MeSOD* genes

The orthologous STRING proteins with the highest bit score were identified using all *MeSOD* protein sequences. Statistical analysis revealed 8 cassava SOD proteins and the homologous proteins match the highest bit score by default, which identified 6 (AtCSD1, AtCSD2, AtCSD3,

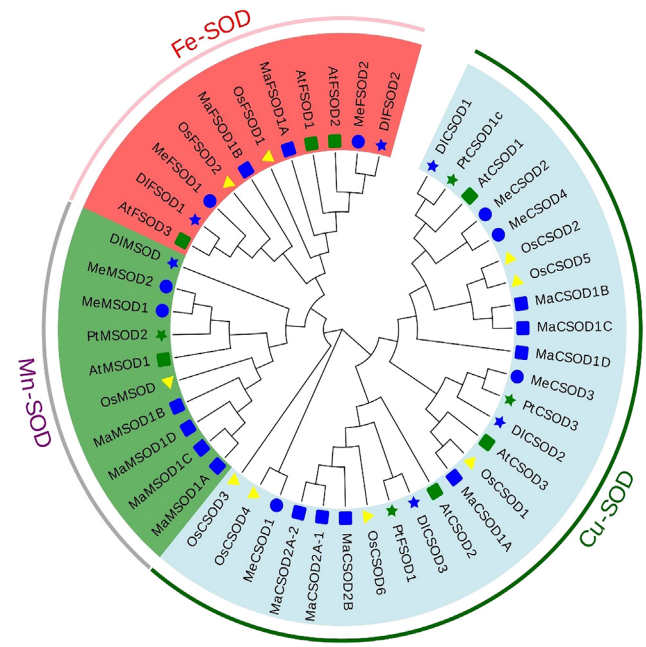

Figure 4. Phylogenetic relationships of *SOD* genes

Phylogenetic relationships of *SOD* genes in *A. thaliana*, *D. longan*, *O. sativa*, *M. acuminata*, *P. trichocarpa*, and *M. esculenta*. All SOD genes were classified into three subfamilies: Cu-SOD, Mn-SOD and Fe-SOD. Neighbor-Joining analysis was performed with a bootstrap value of 1000 using MEGA 7.1 program. Neighbor-joining (NJ) method was used to compute the evolutionary distance. Green square, blue star, yellow triangle, blue square, green star, and blue circle indicate *A. thaliana*, *D. longan*, *O. sativa*, *M. acuminata*, *P. trichocarpa*, and *M. esculenta SODs*, respectively.

AtMSD1, AtFSD1, and AtFSD2) proteins involved in the SOD family networks in *Arabidopsis* (Figure S2). Among the six homologous proteins in *Arabidopsis*, AtFSD1, and AtFSD2 had the most interacting partners (14); all had 10 interacting partners, including members of the SOD gene family, such as CAT, DECOY, and PTAC. These findings may shed light on the functions of unidentified proteins.

Enriched GO terms of the *MeSOD* genes

GO enrichment analysis was conducted to predict the functions of *MeSOD* genes. The GO biological processes showed that four of the eight *MeSOD* genes were associated with "response to stimulus" (GO:0009675). In contrast, the GO molecular function results revealed that four *MeSOD* genes are involved in antioxidant activity (GO:0016209). Besides, *MeSOD* genes participate in metabolic processes and biological regulation. GO enrichment analysis illustrated the functional diversity of *MeSOD* proteins (Figure S3; Table S5).

The secondary and tertiary structures of the *MeSOD* proteins

The three-dimensional model of *MeSOD* genes was predicted using the SWISS-MODEL program (Figure 7), and the modeling templates are listed in Table S6. The quality of the model was verified with Ramachandran plot analysis, which revealed that 80% of the residues were maintained within the allowed area, indicating that the models had a relatively good quality. The predicted secondary structure models were superimposed to determine the structure coverage percentage and assess the generated models' similarity or divergence. The structural coverage percentages of MeCSODs, MeFSODs, and MeMSODs ranged from 70% to 98%, 75%–83%, and 85%–86%, respectively. All *MeSOD* proteins contained α-helices, β-strands, and random coils based on the secondary structure analysis. The tertiary structure analysis of *MeSOD* proteins revealed that all MeCSODs and MeFSODs were homo-dimers except for MeCSOD1. Notwithstanding, all MeMSODs were homo-tetramer. Only MeCSOD1 lacked a ligand, while the remaining *MeSOD* proteins had varying numbers of ligands (Table S6).

Expression of *MeSOD* genes in different tissues and organs

MeSOD genes displayed differential expression in various cassava tissues and were grouped into two groups following the expression levels (Figure 8; Table S7). Group I genes were consistently expressed higher than group II in all these tissues. MeMSOD1 and MeMSOD2 were clustered into I and II, respectively, and showed different tissue-specific expressions in fibrous roots. The highest expression level of MeFSOD2 and MeCSOD4 was found in leaves and brittle calluses, respectively. Group I *MeSOD* genes (MeCSOD2, MeCSOD4, MeFSOD2, and MeMSOD1), exhibited higher expression levels in a specific tissue than the other *MeSOD* genes. MeMSOD1 expression level was significantly higher in sink tissues (e.g., lateral buds, stem apexes), while MeFSOD2 displayed a higher expression level in the leaf and midvein.

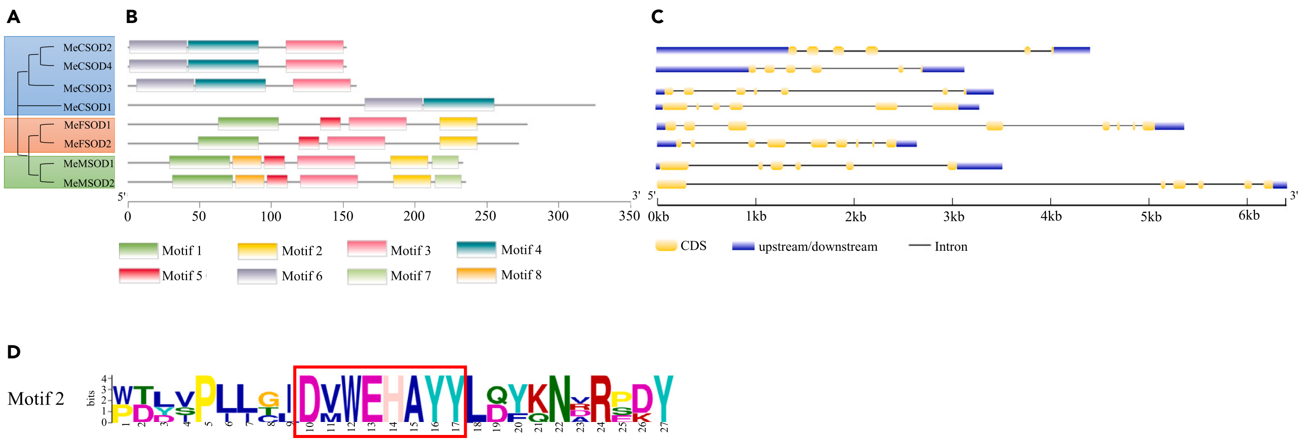

Figure 5. Phylogenetic analysis, gene structure, and conserved motifs of *MeSOD* genes

(A) The phylogenetic tree of *MeSOD* genes. The tree was constructed with a bootstrap of 1000 by the neighbor-joining (NJ) method in MEGA 7.1. *MeSOD* genes of the same class are shown in the same color. Blue represents *CSOD*, orange represents *FSOD*, and green represents *MSODs*.

(B) The motif compositions of *MeSOD* genes were identified by MEME. TBtools was used to visualize the results of motif composition. A specific color indicates each motif.

(C) The gene structure of *MeSOD* genes. Exons and introns are shown with yellow boxes and thin lines, respectively. UTRs are shown in blue boxes.

(D) The conserved motif of *SOD* genes from cassava. The number on the x axis indicates the position of the amino acid. The font sizes indicate their relative frequency at the given position (x axis) in the motif. The red boxes represent the metal-binding motif of the *Fe/Mn-SODs*.

Expression pattern of *MeSOD* genes in response to abiotic stresses and hormones

Previous studies have demonstrated the protective role of the SOD gene family in plants against various abiotic stresses.[51] To investigate the potential roles of *MeSOD* genes in cassava under different abiotic stresses, RNA-seq data were downloaded and analyzed. Additionally, the expression patterns of *MeSOD* genes in response to salt and drought stresses were verified using qRT-PCR.

Under salt stress, the expression profiles of the eight *MeSOD* genes varied (Figure 9A; Table S8). *MeCSOD1* showed a continuous increase in expression, peaking at 6 h and then decreasing at 24 h. In contrast, MeCSOD2 expression steadily increased and peaked at 24 h. MeCSOD3, MeFSOD1, and MeMSOD1 were upregulated at 3 h and downregulated at 6 h. MeCSOD3 and MeFSOD1 exhibited a substantial increase and peaked at 24 h, while MeMSOD1 peaked at 3 h, decreased at 6 h, and slightly increased again at 24 h. Notably, MeMSOD2 was significantly downregulated, remaining nearly unchanged at 1 and 3 h, showing slight expression at 6 h, and remaining unchanged at 24 h. Moreover, MeFSOD2 showed its highest expression level at 24 h, which is particularly interesting as it displayed the highest expression level among all *MeSOD* genes.

To further determine the expression profiles of *MeSOD* genes under abiotic stress, the expression patterns of *MeSOD* genes in roots, stems, and leaves under PEG treatment were investigated using qRT-PCR. The group I genes displayed lower expression than group II (Figure S4; Table S9). MeFSOD1 was consistently expressed at a low level in various tissues, particularly leaves and stems, whereas MeCSOD1 and MeCSOD2, clustered into the same clade in group II, were expressed at a high level in the evaluated tissues. Interestingly, *MeMSOD2* was highly expressed in leaves and stems but barely in roots. *MeSOD* genes were down-regulated in leaves except MeCSOD4, MeFSOD1, and

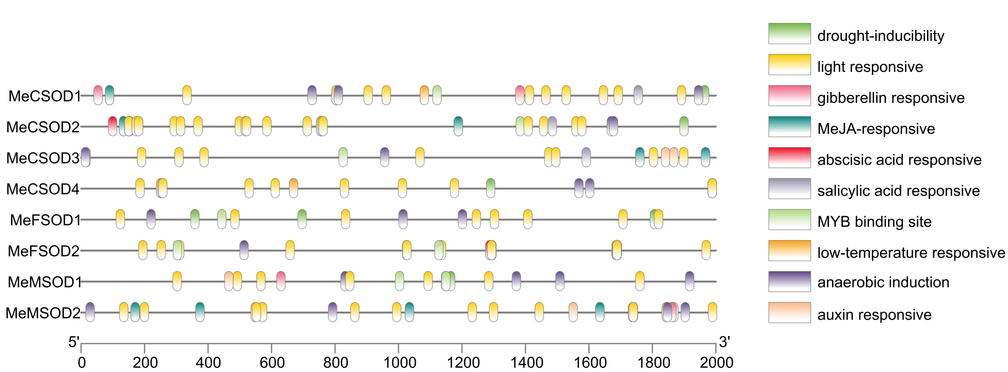

Figure 6. *Cis*-element distribution in putative promoters of *MeSOD* genes

Different *cis*-elements with the same or similar functions are shown in the same color.

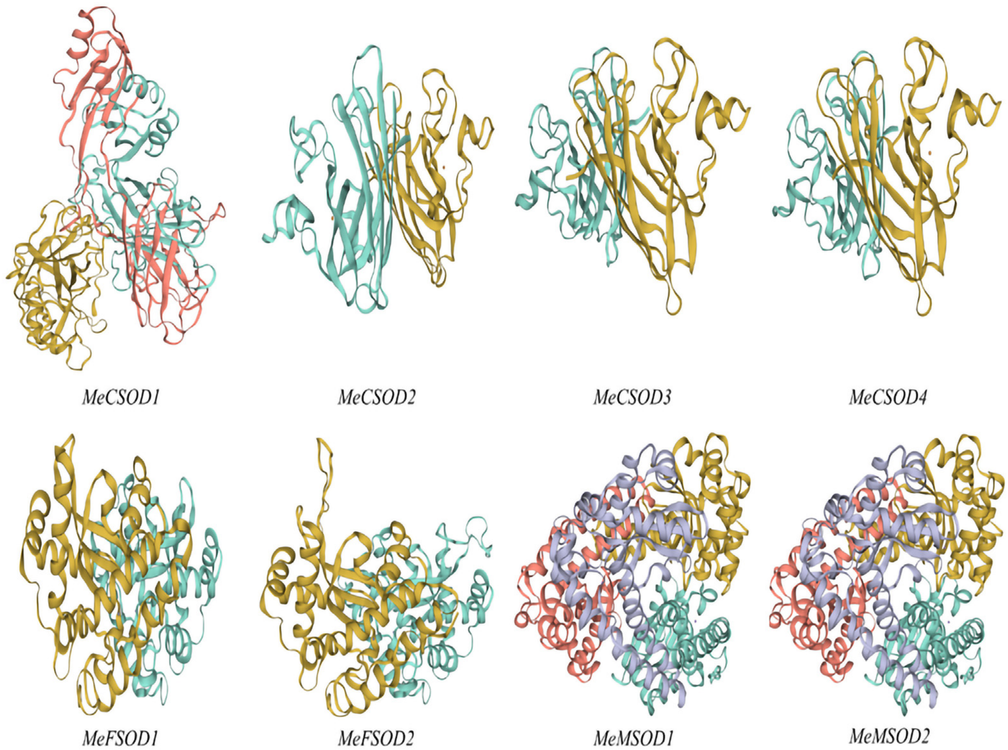

Figure 7. Predicted 3D models of MeSOD proteins
Models were generated by using SWISS MODEL online program. Protein chains were displayed in different colors.

MeMSOD1. Only three *SOD* genes (MeCSOD4, MeFSOD1, and MeMSOD1) were expressed at low levels in the stems, while the rest were upregulated. Two of the eight genes (MeFSOD1 and MeMSOD2) were expressed lower in roots than the others.

Expression pattern of *MeSOD* genes in response to *Xpm*CNH11 infection

The data from NCBI was utilized to predict the expression patterns of *MeSOD* genes in response to CBB infection. *MeSOD* genes displayed different expression patterns in various transcriptome data (Figure S5). Notably, *MeFSOD2* exhibited the highest expression level, peaking at 6 h after infection, while *MeMSOD2* had the lowest expression level, even reaching 0 when not infected (Figure S5A). The expression patterns showed distinct changes after 3 and 6 weeks of infection (Figure S5B). Four genes (MeFSOD1, MeFSOD2, MeMSOD1, MeMSOD2) displayed an increasing trend, while the other four genes (MeCSOD1, MeCSOD2, MeCSOD3, MeCSOD4) exhibited a decreasing trend. However, using another transcriptome dataset, the expression levels showed a different pattern (Figure S5C). Five genes (MeCSOD1, MeCSOD4, MeFSOD1, MeFSOD2, MeMSOD1) increased at 24 h and then decreased at 50 h, while three genes (MeCSOD2, MeCSOD3, MeMSOD2) showed a significant initial decrease followed by a slight increase.

To further verify the disease resistance of *MeSOD* genes, qRT-PCR was employed to analyze their expression patterns against CBB. Interestingly, the qRT-PCR results were not entirely consistent with the transcriptome data, which might be attributed to the differences in the materials used for transcriptome data detection and qRT-PCR analysis. As shown in Figure 9B, MeMSOD2 reached its maximum expression at 3 h, while the expression levels of the other genes peaked at 6 h (Figure 9B; Table S10). However, despite MeMSOD2 having the highest expression level among the *MeSOD* genes, it was observed that MeFSOD2 had a relatively low expression level, contrary to the results of the expression patterns in the transcriptome data. Among the eight genes, MeCSOD1, MeCSOD2, MeCSOD4, and MeMSOD1 exhibited similar expression patterns, increasing steadily at 1 day, 3 days, and 6 days. However, MeCSOD3, MeFSOD2, and MeMSOD2 showed a slight down-regulation on the third day and a brief upregulation on the sixth day. Additionally, MeFSOD1 displayed a decrease on the first day, a slight increase on the third day, and another decrease on the sixth day.

VIGS confirms MeMSOD2's resistance to CBB

After 30 days of infection, the positive control plants exhibited whitening and yellowing of new leaves, while both the negative control and the experimental group containing the pCsCMV-MeMSOD2 recombinant plasmid showed no changes in the leaves. This indicates that the pCsCMV-NC system effectively silenced the endogenous *ChlI* gene in cassava. Total RNA was extracted from cassava new leaves of the experimental group, and the negative control, and after reverse transcription into cDNA, the silencing efficiency of the target

CellPress
OPEN ACCESS

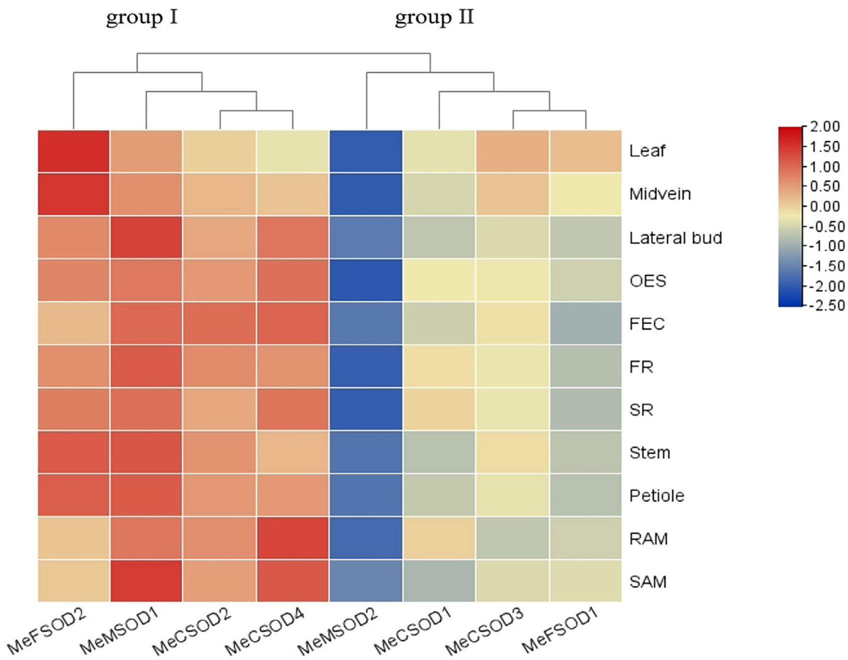

Figure 8. Heatmap representation and hierarchical clustering of the *MeSOD* genes in various cassava tissues
Expressions of 8 *MeSOD* genes in leaves, midveins, lateral buds, somatic embryos (OES), brittle calluses (FEC), fibrous roots (FR), root tubers (SR), stems, petioles, root tips (RAM), stem apexes (SAM) were tested. The bar at the right of the heatmap represents the relative expression values; values <0 represent downregulated expression, and values >0 represent upregulated expression.

gene was determined using qRT-PCR. Each group's data came from 3 biological replicates (Figure 10A). Compared with the negative control plants, the expression level of MeMSOD2 in new leaves of silenced plants significantly decreased, confirming the effective silencing of the MeMSOD2 gene.

To verify the function of MeMSOD2 in resistance to CBB, water-stained lesions appeared on the leaves of both MeMSOD2-silenced plants and negative control plants after 3 days of inoculation, but the spread area of disease spots on MeMSOD2-silenced plants was larger. After 6 days of infection, the lesion area of MeMSOD2-silenced plants further expanded, while the lesion area of negative control plants expanded slowly (Figure 10B).

For quantification of the lesion area, ImageJ software[52] was used to calculate the lesion area after 3 and 6 days of infection with *Xpm*CHN11, and a histogram was created for significance analysis (Figure 10C). After 3 days of inoculation, the lesion area of MeMSOD2-silenced plants slightly increased compared to the negative control plants. After 6 days of inoculation, the lesion area of MeMSOD2-silenced plants was again higher than that of the negative control plants. These results indicate that the sensitivity of cassava to *Xpm*CHN11 increased after silencing the MeMSOD2 gene.

DISCUSSION

SOD genes act as the first line of defense in the antioxidant system, responding to various environmental cues and protecting plants from the damage caused by toxic ROS.[53,54] To our best knowledge, the comprehensive characterization of the SOD gene family in cassava has not been reported. Hence, identifying SOD gene family members in cassava could provide invaluable references for future functional genetic studies and support efforts to genetically improve stress tolerance in cassava. The present study identified eight SOD genes in the cassava genome, including 4 CSODs, 2 FSODs, and 2 MSODs (Table 1). The gene number of SOD varies in different species. For instance, *Arabidopsis*, *Gossypium hirsutum*, and *T. aestivum* contained 7, 18, and 23 genes, respectively.[21,51,55] All found MeCSODs contained a conserved SOD-Cu domain (Pfam: 00080). However, the MeCSOD1 contained an additional HMA domain (Pfam: PF00403). In addition, the MeFSODs and MeMSODs contained a SOD-Fe/Mn domain (Pfam: 02777 and Pfam: 00081). These results support the hypothesis that SOD proteins are highly conserved in eukaryotes.[56] Moreover, the number of *MeSOD* genes is consistent with previous results. For instance, rice, tea plant (*Camellia sinensis*), and foxtail millet (*Setaria italica* P. Beauv.) contained eight (5 CSODs, 2 FSODs, and 1 MSOD), eight (4 CSODs, 3 FSODs, and 1 MSOD), and eight (4 CSODs, 3 FSODs, and 1 MSOD) SOD genes, respectively.[57–59] But less or more SOD genes than *A. thaliana* (7), *Larix kaempferi* (6), *S. lycopersicum* (9), *C. sinensis* (10), and *Cucumis sativus* (9).[21,23,25,59] The variation in SOD family member numbers may be due to the different genome sizes of different species.[60]

Phylogenetic analysis revealed that FSODs and MSODs members were closely related but separated from CSODs (Figure 4), indicating that FSODs and MSODs might share the same ancestor based on the bootstrap values.[59] Previous studies reported that only MSOD and

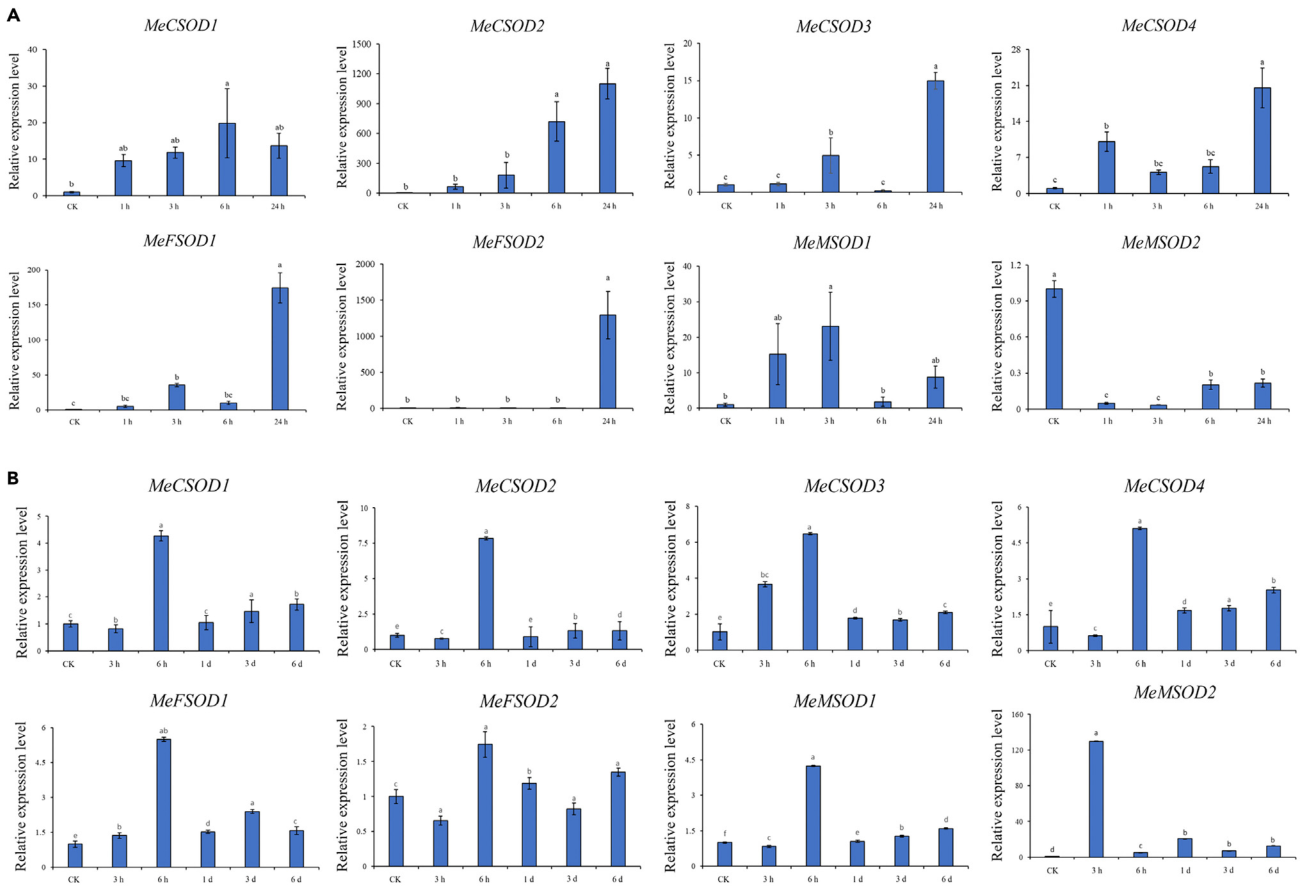

Figure 9. *MeSOD* gene expression profiles in response to NaCl treatment and *Xanthomonas phaseoli* pv. *manihotis* (*Xpm*)

(A and B) Quantitative real-time PCR (qRT-PCR) analysis of *MeSOD* genes in salinity (A) and cassava bacterial blight (B) treatments. Expression data were normalized using *MeEF1α* as the internal control, and error bars indicate the standard deviation among three biological replicates. "a": extremely significant difference; "b": significant difference; "c-e": zero difference. The significant difference analysis marks are only applicable to the same histogram.

FSOD exist in algae and bryophytes, implying they evolved first.[26] *MeSOD* gene members within the same subgroup tended to be predicted in the same cellular compartments, consistent with the finding that SOD gene clustering is related to subcellular localization.[53,58] MeCSOD2, MeCSOD3, and MeCSOD4 were clustered into the same subgroup and were predicted to be cytoplasmic, whereas MeCSOD1 was clustered into a different subgroup and was predicted to be chloroplastic (Table 1; Figure 4). Notably, *MeSODs* sharing the same clade showed similar protein structures, such as MeMSOD1 and MeMSOD2 (Figure 7). The conserved motif analysis supported the result of the phylogenetic analysis (Figure 5). *MeSODs* belonging to the same subgroups shared common motifs and similar positions and lengths (Figure 5; Table S3). In addition, gene structure analysis showed distinct intron numbers in the *MeSOD* genes (Figure 5). Exon-intron structural diversity frequently plays a key role in the evolution of gene families and provides additional evidence to support evolutionary relationships.[61,62] It was reported that plant SOD genes have highly conserved patterns, and many cytosolic and chloroplastic SODs possess seven introns.[63] The intron numbers ranged from five to eight in *MeSOD* genes. Only MeFSOD1, predicted to be a chloroplastic SOD gene, contained seven introns (Table S4). Other cytosolic and chloroplastic *MeSOD* genes contained five to six introns. MeCSOD1, MeCSOD2, and MeCSOD4 had five introns. Three main mechanisms, exon/intron, gain/loss, exonization/pseudoexonization, and insertion/deletion, lead to the variation in intron-exon number and result in structural divergence in various genes.[64] Moreover, it was reported that gene structure and conserved sequence construction might be closely related to the diversity of gene function, including enzymatic activity and expression pattern in response to various stresses.[65]

A crucial way to expand the gene families and provide new genetic material and novel genes is gene duplication, including tandem duplication, tetraploidy, segmental duplication, and single gene transposition-duplication.[66–71] Gene duplication analysis revealed that all the gene duplication events (MeCSOD2/MeCSOD4 and MeMSOD1/MeMSOD2) were segmental and present in the same clade of the phylogenetic tree, consistent with the results from *Gossypium* (Figures 2 and 4).[24] However, in grapevine (*Vitis vinifera*), *VvCSOD4*/*VvCSOD5* was a tandemly duplicated gene pair, while *VvMSOD1*/*VvMSOD2* was a segmentally duplicated gene pair.[28]

Cis-elements subsidize plant stress responses.[72,73] Most *MeSOD* promoters were stress-responsive *cis*-elements related to drought, low-temperature, and hormone-responsive *cis*-elements (Figure 6). In addition, six of the 8 *MeSOD* genes contained MYB binding sites.

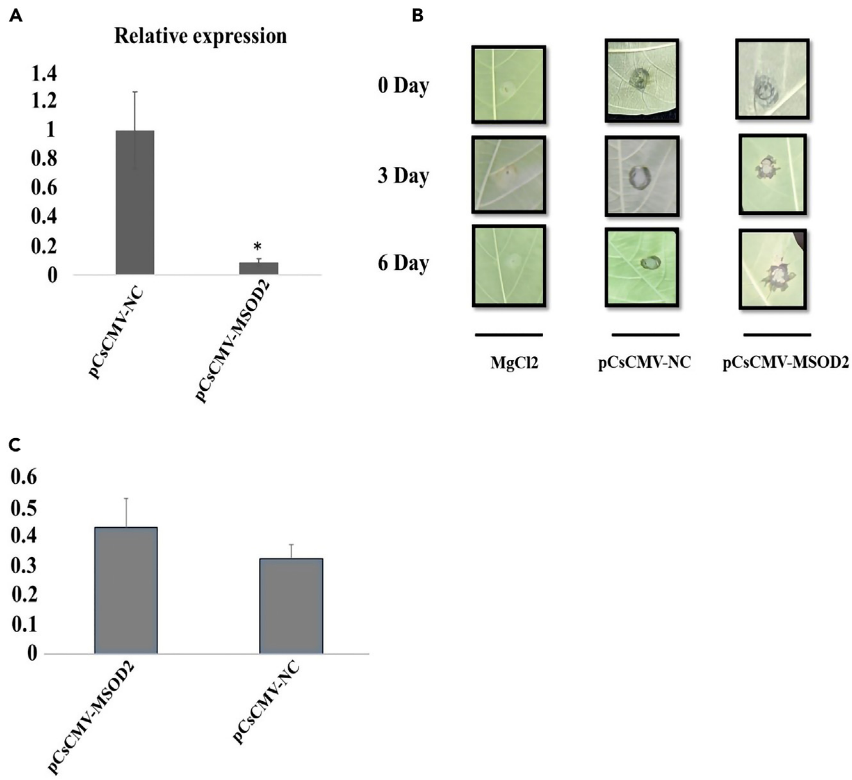

Figure 10. Phenotypic characteristics of bacteria infecting cassava leaves after Xpm inoculation

(A) qRT-PCR validation of MSOD2 silencing efficiency, pCsCMV-NC represents negative control.

(B) The phenotypes of cassava leaves infected with XpmCHN11 after inoculation with pCsCMV-MSOD2, an empty vector (pCsCMV-NC), and 10 mM MgCl2 (Mock).

(C) The lesion area of cassava leaves was calculated using the ImageJ tool at 200 pixels per centimeter resolution. Note: *: indicate the significance differences ($p < 0.05$).

MYB transcription factors are critical in plants' growth and defense responses.[74] The presence of MYB-related *cis*-elements in high abundance in *MeSOD* genes suggested that it may be involved in regulating the level of *MeSOD* gene expression in response to environmental stresses. The drought-responsive element was the most widely distributed in five genes (MeCSOD1, MeCSOD2, MeCSOD4, MeFSOD1, and MeMSOD1), except the MYB binding site. The widespread distribution of drought-responsive elements suggests they might be involved in drought stress. PPI showed that CAT was in the center of the interaction network, interacting with CSD1, CSD2, CSD3, FSD1, FSD2, and MSD1. In the present study, MeCSOD2 and MeCSOD4 were syntenic paralogs of CSD1 in cassava; MeMSOD1 and MeMSOD2 were syntenic paralogs of CSD2; MeCSOD3 was syntenic paralog of CSD3; MeFSOD2 was syntenic paralog of FSD1 and FSD2, and MeMSOD1 was syntenic paralog of MSD1. CAT is a powerful antioxidant metalloenzyme mainly located in peroxisomes, which ROS could modulate. The result indicated that *MeSOD* genes might interact with CAT and contribute significantly to antioxidative metabolism, either with CAT or alone.

The miRNAs, a diverse category of nuclear-encoded small RNAs, play multiple and central functions in plant development, stress responses, and many other biological processes. Five *MeSOD* genes were predicted to target 17 miRNAs from four different miRNA families. Among them, *mes-miR319b* was represented as the first putative mirtron demonstrated in cassava.[75] A pair of sense and antisense miRNAs, *mes-miR395a* and *mes-miR395b*, targeted MeFSOD1. Reports on the miR319 family suggested that this family was involved in the jasmonic acid signaling pathway regulated by bacteria.[76] We hypothesised that MeCSOD3, targeting seven miR319 family members (*mes-miR319a* to *mes-miR319g*), may regulate cassava response to bacterial pathogen infection.

The SODs act as one of the most effective components of the antioxidant defense system in plant cells and are related to protecting plants from environmental stresses. For instance, *A. thaliana* contained three SOD genes that respond to oxidative stresses, including ozone fumigation and UV-B illumination.[21] Mitochondrial MSOD1 in sunflower (*Helianthus annuus* L.), which was sensitive and could act as an early sensor of adverse conditions, shows significant upregulation under low-temperature stress.[77] The expression level of CSODs in *Caragana* (*Caragana* Fabr.) indicated that three CSODs play a crucial role in response to water stress.[78] In triticale (*Triticosecale wittmack*), CSOD and MSOD are the most important antioxidant enzymes against drought stress.[79] Moreover, the transgenic plants displayed the same effect. For example, the transgenic tobacco (*Nicotiana tabacum* L.) expressed a chimeric gene encoding chloroplast-localized CSOD from peas under chilling temperatures and moderate or high light intensity to reduce levels of light-mediated cellular damage.[80] The transgenic plum (*Prunus domestica*) overexpressed cytoplasmic SOD encoding CSOD in the cytosol, making it more tolerant to salt stress.[81] The transgenic cassava that overproduced MeCSOD is resistant to *T. cinnabarinus* (Boisduval).[34]

Various abiotic stresses, such as waterlogging and salt stress, challenge plants' growth and development, producing ROS.[82–84] A previous study indicated that the special role of SOD genes in the development and biological function of different tissues could be implied by the preferential expression pattern of SOD genes.[50] Overexpression of genes that encode different isoforms of SOD can confer resistance to various plant abiotic stresses. For instance, overexpression of a Cu/ZnSOD from *Puccinellia tenuiflora* (PutCu/Zn-SOD) conferred tolerance to several abiotic stresses in transgenic *Arabidopsis*.[85] Hence, we investigated the tissue-specific expression levels of *MeSOD* genes in 11 tissues, demonstrating that *MeSOD* genes showed tissue-specific expression patterns (Figure 8). Interestingly, the segmentally duplicated gene pairs (*MeCSOD2/MeCSOD4*) displayed similar expression patterns in all 11 tissues. However, the segmentally duplicated gene pair, *MeMSOD1/MeMSOD2*, was divided into groups and displayed different expression patterns in all tissues. The same results were reported for upland cotton and wheat.[29,55] It was suggested that a duplication pattern attributable to the expression divergence hinted at a different evolutionary course of duplicated genes.[86]

The expression levels of *MeSOD* genes under salt stress were analyzed (Figure 9A). *MeCSOD2* was strongly activated, and the expression levels of *MeCSOD2* increased on time. However, *MeFSOD2* was expressed lately but showed the highest expression level among *MeSOD* genes, suggesting the crucial roles of *MeCSOD2* and *MeFSOD2* in salt resistance. In particular, the resistance of *MeCSOD2* to salt stress may increase over time. Three special tissues were sampled and assessed for PEG treatment at different time points (Figure S4). *MeFSOD1* had the lowest expression in all three tissues compared to other genes. Interestingly, *MeMSOD2* was highly expressed in response to PEG treatment, indicating that *MeMSOD2* may play an important role in leaves responding to abiotic stress but may have other functions in roots. A similar phenomenon was observed in upland cotton (*G. hirsutum*).[55] Besides, *MeFSOD1*, which exhibited consistently low expression in PEG treatment, may have other functions in cassava rather than coping with stress. The segmental duplication gene pairs, *MeCSOD2/MeCSOD4* and *MeMSOD1/MeMSOD2*, displayed distinct expression patterns in response to PEG treatment.

The SOD gene family also plays a role in response to CBB, which seriously impacts cassava production.[87–91] The scientific literature reviewed the mechanism of plant response to CBB.[92,93] Plant melatonin biosynthesis genes and endogenous melatonin levels that positively regulate plant disease resistance are regulated by common and upstream transcription actors, *MeRAV1* and *MeRAV2*, enabling plants to fight CBB.[92] Besides, the basic domain-leucine zipper (bZIP) transcription factor in cassava is also essential for combating CBB.[93] In the present study, the expression patterns of *MeSOD* genes under CBB were detected (Figure 9B). The expression levels of 8 *MeSOD* genes were relatively similar and stable, except for *MeFSOD2* and *MeMSOD2*. The response of *MeMSOD2* was relatively high among all genes, indicating that *MeMSOD2* may contribute to CBB resistance. Interestingly, the expression level of *MeCSOD3* reached a peak at 6 h, then rapidly decreased over time. The results contradicted the hypothesis that *MeCSOD3* was related to bacterial pathogen infection. The analysis above revealed that *MeSOD* genes are associated with diverse functions under biotic stress.

VIGS is a convenient and effective reverse genetics technique that allows for the silencing of target genes in plants by constructing recombinant viral vectors. Numerous plant virus vectors have been developed to silence genes in various plant tissues[94,95] successfully employed the cassava Common Mosaic Virus (CsCMV) to establish a new VIGS system, pCsCMV-NC, suitable for cassava. Similarly, WEI et al., utilized the tobacco rattle virus (TRV)-mediated silencing system to silence the cassava MeHsf20 and MeWRKY79 genes, reducing melatonin levels and disease resistance in plants.[96] This study used the PCSCMV-NC-mediated VIGS technique to silence the cassava *MeMSOD2* gene. RT-qPCR results indicated a significant reduction in the expression level of the *MeMSOD2* gene in the leaves of the experimental group, confirming effective gene silencing (Figure 10). Subsequently, we observed a notable decrease in cassava's resistance to bacterial blight after inoculating the MeMSOD2-silenced cassava plants with *Xpm*CHN11 pathogens.

Limitations of the study

Subcellular localization and functional analysis of MeCSODs, MeFSODs, and MeMSOD1 could offer comprehensive insights into SOD genes and shed light on their potential functions in environmental stress tolerance. Additionally, studies have reported that combined SOD plays a crucial role in cassava under cold and drought stresses. Hence, investigating the combined SOD in cassava could also provide valuable insights into SOD genes.

STAR★METHODS

Detailed methods are provided in the online version of this paper and include the following:

- KEY RESOURCES TABLE
- RESOURCE AVAILABILITY
  - Lead contact
  - Material availability
  - Data and code availability
- EXPERIMENTAL MODEL AND STUDY PARTICIPANT DETAILS
- METHOD DETAILS
  - Identification and sequence analyses of SOD gene family in cassava

- ○ Phylogenetic relationship, conserved motif, and gene structure analysis
- ○ Chromosomal location, whole-genome duplication, and synteny analysis
- ○ Regulatory elements analysis of *MeSOD* genes and prediction of miRNA targets
- ○ Protein-protein interaction (PPI) network of MeSOD genes
- ○ GO annotation and tissue-specific expression profile of MeSOD genes
- ○ Expression pattern profiling of MeSODs under various abiotic stresses
- ○ Construction of VIGS vector of *MeMSOD2* and infection of 'SC8' cassava
- QUANTIFICATION AND STATISTICAL ANALYSIS

SUPPLEMENTAL INFORMATION

Supplemental information can be found online at https://doi.org/10.1016/j.isci.2023.107801.

ACKNOWLEDGMENTS

We thank the reviewers and editors for their patience and continuous hard striving. This work was supported by the earmarked funding for the China Agricultural Research System (CARS-11-HNCYH), National Natural Science Foundation of China (32260468).

AUTHOR CONTRIBUTIONS

L.Z., A.H.A., K.L., and Y.C. conceived the study and worked on approving the manuscript. L.Z., A.H.A., X.Zhao, and H.L. performed the experiments and wrote the first draft. L.Z., A.H.A., X.Zhao, K.L., Y.C., Z.O., and X.Zhang revised the manuscript. L.Z., A.H.A., and J.L. contributed to data analysis and managed reagents. All authors contributed to the article and approved it for publication.

DECLARATION OF INTERESTS

The authors declare no competing interests.

Received: December 27, 2022
Revised: July 29, 2023
Accepted: August 29, 2023
Published: September 27, 2023

REFERENCES

1. Gull, A., Lone, A.A., and Wani, N.U. (2019). Biotic and Abiotic Stresses in Plants, pp. 1–19.
2. Foyer, C.H., and Noctor, G. (2005). Redox homeostasis and antioxidant signaling: a metabolic interface between stress perception and physiological responses. Plant Cell *17*, 1866–1875. https://doi.org/10.1105/tpc.105.033589.
3. Quan, L.J., Zhang, B., Shi, W.W., and Li, H.Y. (2008). Hydrogen peroxide in plants: a versatile molecule of the reactive oxygen species network. J. Integr. Plant Biol. *50*, 2–18. https://doi.org/10.1111/j.1744-7909.2007.00599.x.
4. Hernández, J.A., Ferrer, M.A., Jiménez, A., Barceló, A.R., and Sevilla, F. (2001). Antioxidant systems and O2.−/H2O2 production in the apoplast of pea leaves. Its relation with salt-induced necrotic lesions in minor veins. Plant Physiol. *127*, 817–831. https://doi.org/10.1104/pp.010188.
5. Stephenie, S., Chang, Y.P., Gnanasekaran, A., Esa, N.M., and Gnanaraj, C. (2020). An insight on superoxide dismutase (SOD) from plants for mammalian health enhancement. J. Funct.Foods *68*, 103917. https://doi.org/10.1016/j.jff.2020.103917.
6. Palma, J.M., Mateos, R.M., López-Jaramillo, J., Rodríguez-Ruiz, M., González-Gordo, S., Lechuga-Sancho, A.M., and Corpas, F.J. (2020). Plant catalases as NO and H2S targets. Redox Biol. *34*, 101525. https://doi.org/10.1016/j.redox.2020.101525.
7. Bhatt, I., and Tripathi, B.N. (2011). Plant peroxiredoxins: catalytic mechanisms, functional significance and future perspectives. Biotechnol. Adv. *29*, 850–859. https://doi.org/10.1016/j.biotechadv.2011.07.002.
8. Margis, R., Dunand, C., Teixeira, F.K., and Margis-Pinheiro, M. (2008). Glutathione peroxidase family–an evolutionary overview. FEBS J. *275*, 3959–3970. https://doi.org/10.1111/j.1742-4658.2008.06542.x.
9. Alscher, R.G., Erturk, N., and Heath, L.S. (2002). Role of superoxide dismutases (SODs) in controlling oxidative stress in plants. J. Exp. Bot. *53*, 1331–1341. https://doi.org/10.1093/jexbot/53.372.1331.
10. Lin, K.H., Sei, S.-C., Su, Y.H., and Chiang, C.M. (2019). Overexpression of the *Arabidopsis* and winter squash superoxide dismutase genes enhances chilling tolerance via ABA-sensitive transcriptional regulation in transgenic *Arabidopsis*. Plant Signal. Behav. *14*, 1685728. https://doi.org/10.1080/15592324.2019.1685728.
11. McCord, J.M., and Fridovich, I. (1969). Superoxide dismutase: an enzymic function for erythrocuprein (hemocuprein). J. Biol. Chem. *244*, 6049–6055. https://doi.org/10.1016/S0021-9258(18)63504-5.
12. Youn, H.D., Kim, E.-J., Roe, J.H., HAH, Y.C., and KANG, S.O. (1996). A novel nickel-containing superoxide dismutase from Streptomyces spp. Biochem. J. *318*, 889–896. https://doi.org/10.1042/bj3180889.
13. Miller, A.F. (2001). Fe superoxide dismutase. Handbook Metalloproteins *1*, 668–682.
14. Xia, M., Wang, W., Yuan, R., Den, F., and Shen, F. (2015). Superoxide dismutase and its research in plant stress-tolerance *13*, 2633–2646.
15. Wuerges, J., Lee, J.W., Yim, Y.I., Yim, H.S., Kang, S.O., and Djinovic Carugo, K. (2004). Crystal structure of nickel-containing superoxide dismutase reveals another type of active site. Proc. Natl. Acad. Sci. USA *101*, 8569–8574. https://doi.org/10.1073/pnas.0308514101.
16. Kim, F.J., Kim, H.P., Hah, Y.C., and Roe, J.H. (1996). Differential expression of superoxide dismutases containing Ni and Fe/Zn in Streptomyces coelicolor. Eur. J. Biochem. *241*, 178–185. https://doi.org/10.1111/j.1432-1033.1996.0178t.x.
17. Chen, Z.J., Scheffler, B.E., Dennis, E., Triplett, B.A., Zhang, T., Guo, W., Chen, X., Stelly, D.M., Rabinowicz, P.D., Town, C.D., et al. (2007). Toward sequencing cotton (*Gossypium*) genomes. Plant Physiol. *145*, 1303–1310. https://doi.org/10.1104/pp.107.107672.
18. Kanematsu, S., and Asada, K. (1990). Characteristic amino acid sequences of chloroplast and cytosol isozymes of CuZn-superoxide dismutase in spinach, rice and horsetail. Plant Cell Physiol. *31*, 99–112.

https://doi.org/10.1093/oxfordjournals.pcp.a077887.
19. Smith, M.W., and Doolittle, R.F. (1992). A comparison of evolutionary rates of the two major kinds of superoxide dismutase. J. Mol. Evol. *34*, 175–184. https://doi.org/10.1007/BF00182394.
20. Xu, J., Duan, X., Yang, J., Beeching, J.R., and Zhang, P. (2013). Coupled expression of Cu/Zn-superoxide dismutase and catalase in cassava improves tolerance against cold and drought stresses. Plant Signal. Behav. *8*, e24525. https://doi.org/10.4161/psb.24525.
21. Kliebenstein, D.J., Monde, R.-A., and Last, R.L. (1998). Superoxide dismutase in *Arabidopsis*: an eclectic enzyme family with disparate regulation and protein localization. Plant Physiol. *118*, 637–650. https://doi.org/10.1104/pp.118.2.637.
22. Feng, X., Lai, Z., Lin, Y., Lai, G., and Lian, C. (2015). Genome-wide identification and characterization of the superoxide dismutase gene family in Musa acuminata cv. Tianbaojiao (AAA group). BMC Genom. *16*, 823–916. https://doi.org/10.1186/s12864-015-2046-7.
23. Feng, K., Yu, J., Cheng, Y., Ruan, M., Wang, R., Ye, Q., Zhou, G., Li, Z., Yao, Z., Yang, Y., et al. (2016). The SOD gene family in tomato: identification, phylogenetic relationships, and expression patterns. Front. Plant Sci. *7*, 1279. https://doi.org/10.3389/fpls.2016.01279.
24. Zhang, J., Li, B., Yang, Y., Hu, W., Chen, F., Xie, L., and Fan, L. (2016). Genome-wide characterization and expression profiles of the superoxide dismutase gene family in *Gossypium*. Int. J. Genomics *2016*, 8740901. https://doi.org/10.1155/2016/8740901.
25. Zhou, Y., Hu, L., Wu, H., Jiang, L., and Liu, S. (2017). Genome-wide identification and transcriptional expression analysis of cucumber superoxide dismutase (SOD) family in response to various abiotic stresses. Int. J. Genomics *2017*, 7243973. https://doi.org/10.1155/2017/7243973.
26. Lin, Y.L., and Lai, Z.X. (2013). Superoxide dismutase multigene family in longan somatic embryos: a comparison of CuZn-SOD, Fe-SOD, and Mn-SOD gene structure, splicing, phylogeny, and expression. J. Mol. Biol. *32*, 595–615. https://doi.org/10.1007/s11032-013-9892-2.
27. Wang, T., Song, H., Zhang, B., Lu, Q., Liu, Z., Zhang, S., Guo, R., Wang, C., Zhao, Z., Liu, J., et al. (2018). Genome-wide identification, characterization, and expression analysis of superoxide dismutase (SOD) genes in foxtail millet (*Setaria italica* L.). 3 Biotech *8*, 486–511. https://doi.org/10.1007/s13205-018-1502-x.
28. Hu, X., Hao, C., Cheng, Z.M., and Zhong, Y. (2019). Genome-wide identification, characterization, and expression analysis of the grapevine superoxide dismutase (SOD) family. Int. J. Genomics *2019*, 7350414. https://doi.org/10.1155/2019/7350414.
29. Jiang, W., Yang, L., He, Y., Zhang, H., Li, W., Chen, H., Ma, D., and Yin, J. (2019). Genome-wide identification and transcriptional expression analysis of superoxide dismutase (SOD) family in wheat (*Triticum aestivum*). PeerJ *7*, e8062. https://doi.org/10.7717/peerj.8062.
30. Verma, D., Lakhanpal, N., and Singh, K. (2019). Genome-wide identification and characterization of abiotic-stress responsive SOD (superoxide dismutase) gene family in *Brassica juncea* and *B. rapa*. BMC Genom. *20*, 227–318. https://doi.org/10.1186/s12864-019-5593-5.
31. Pilon, M., Ravet, K., and Tapken, W. (2011). The biogenesis and physiological function of chloroplast superoxide dismutases. Biochim. Biophys. Acta *1807*, 989–998. https://doi.org/10.1016/j.bbabio.2010.11.002.
32. Asensio, A.C., Gil-Monreal, M., Pires, L., Gogorcena, Y., Aparicio-Tejo, P.M., and Moran, J.F. (2012). Two Fe-superoxide dismutase families respond differently to stress and senescence in legumes. J. Plant Physiol. *169*, 1253–1260. https://doi.org/10.1016/j.jplph.2012.04.019.
33. Kaouthar, F., Ameny, F.K., Yosra, K., Walid, S., Ali, G., and Faiçal, B. (2016). Responses of transgenic *Arabidopsis* plants and recombinant yeast cells expressing a novel durum wheat manganese superoxide dismutase TdMnSOD to various abiotic stresses. J. Plant Physiol. *198*, 56–68. https://doi.org/10.1016/j.jplph.2016.03.019.
34. Lu, F., Liang, X., Lu, H., Li, Q., Chen, Q., Zhang, P., Li, K., Liu, G., Yan, W., Song, J., et al. (2017). Overproduction of superoxide dismutase and catalase confers cassava resistance to *Tetranychus cinnabarinus*. Sci. Rep. *7*, 40179–40213. https://doi.org/10.1038/srep40179.
35. Olsen, K.M., and Schaal, B.A. (1999). Evidence on the Origin of Cassava: Phylogeography of Manihot esculenta. P Natl Acad Sci USA *96*, 5586–5591. https://doi.org/10.1073/pnas.96.10.558.
36. El-Sharkawy, M.A. (2004). Cassava biology and physiology. Plant Mol. Biol. *56*, 481–501. https://doi.org/10.1007/s11103-005-2270-7.
37. Papong, S., and Malakul, P. (2010). Life-cycle energy and environmental analysis of bioethanol production from cassava in Thailand. Bioresour. Technol. *101*, S112–S118. https://doi.org/10.1016/j.biortech.2009.09.006.
38. Zidenga, T., Leyva-Guerrero, E., Moon, H., Siritunga, D., and Sayre, R. (2012). Extending cassava root shelf life via reduction of reactive oxygen species production. Plant Physiol. *159*, 1396–1407. https://doi.org/10.1104/pp.112.200345.
39. Hu, W., Wei, Y., Xia, Z., Yan, Y., Hou, X., Zou, M., Lu, C., Wang, W., and Peng, M. (2015). Genome-wide identification and expression analysis of the NAC transcription factor family in cassava. PLoS One *10*, e0136993. https://doi.org/10.1371/journal.pone.0136993.
40. Ding, Z., Fu, L., Yan, Y., Tie, W., Xia, Z., Wang, W., Peng, M., Hu, W., and Zhang, J. (2017). Genome-wide characterization and expression profiling of HD-Zip gene family related to abiotic stress in cassava. PLoS One *12*, e0173043. https://doi.org/10.1371/journal.pone.0173043.
41. Lozano, J.C. (1986). Cassava bacterial blight: a manageable disease. Plant Dis. *70*, 1089–1993.
42. Lozano, J.C., and Sequiera, L. (1974). Bacterial blight of cassava in Colombia: epidemiology and control. Phytopathology *64*, 83–88.
43. López, C.E., and Bernal, A.J. (2012). Cassava bacterial blight: using genomics for the elucidation and management of an old problem. Trop. Plant Biol. *5*, 117–126. https://doi.org/10.1007/s12042-011-9092-3.
44. Joseph, J., and Elango, F. (1991). The status of cassava bacterial blight caused by *Xanthomonas campestris pv. manihotis* in Trinidad. J. Phytopathol. *133*, 320–326. https://doi.org/10.1111/j.1439-0434.1991.tb00167.x.
45. Koné, D., Dao, S., Tekete, C., Doumbia, I., Koita, O., Abo, K., Wicker, E., and Verdier, V. (2015). Confirmation of *Xanthomonas axonopodis pv. manihotis* causing cassava bacterial blight in Ivory Coast. Plant Dis. *99*, 1445.
46. Wonni, I., Ouedraogo, L., Dao, S., Tekete, C., Koita, O., Taghouti, G., Portier, P., Szurek, B., and Verdier, V. (2015). First report of cassava bacterial blight caused by *Xanthomonas axonopodis pv. manihotis* in Burkina Faso. Plant Dis. *99*, 551. https://doi.org/10.1094/PDIS-03-14-0302-PDN.
47. Bredeson, J.V., Lyons, J.B., Prochnik, S.E., Wu, G.A., Ha, C.M., Edsinger-Gonzales, E., Grimwood, J., Schmutz, J., Rabbi, I.Y., Egesi, C., et al. (2016). Sequencing wild and cultivated cassava and related species reveals extensive interspecific hybridization and genetic diversity. Nat. Biotechnol. *34*, 562–570. https://doi.org/10.1038/nbt.3535.
48. Huang, S., Tang, Z., Zhao, R., Hong, Y., Zhu, S., Fan, R., Ding, K., Cao, M., Luo, K., Geng, M., et al. (2021). Genome-wide identification of cassava MeRboh genes and functional analysis in Arabidopsis. J. Plant Pathol. *167*, 296–308. https://doi.org/10.3390/plants9111452.
49. Prochnik, S., Marri, P.R., Desany, B., Rabinowicz, P.D., Kodira, C., Mohiuddin, M., Rodriguez, F., Fauquet, C., Tohme, J., Harkins, T., et al. (2012). The cassava genome: current progress, future directions. Trop. Plant Biol. *5*, 88–94. https://doi.org/10.1007/s12042-011-9088-z.
50. Huang, H., Wang, H., Tong, Y., and Wang, Y. (2020). Insights into the superoxide dismutase gene family and its roles in *dendrobium catenatum* under abiotic stresses. J. Plant *9*, 1452. https://doi.org/10.3390/plants9111452.
51. Tyagi, S., Sharma, S., Taneja, M., Kumar, R., Kumar, R., Sembi, J.K., and Upadhyay, S.K. (2017). Superoxide dismutases in bread wheat (*Triticum aestivum* L.): comprehensive characterization and expression analysis during development and, biotic and abiotic stresses. Agri Gene *6*, 1–13. https://doi.org/10.1016/j.aggene.2017.08.003.
52. Schneider, C.A., Rasband, W.S., and Eliceiri, K.W. (2012). NIH Image to ImageJ: 25 years of image analysis. Nat. Methods *9*, 671–675. https://doi.org/10.1038/nmeth.2089.
53. Song, J., Zeng, L., Chen, R., Wang, Y., and Zhou, Y. (2018). In silico identification and expression analysis of superoxide dismutase (SOD) gene family in *Medicago truncatula*. 3 Biotech *8*, 348–412. https://doi.org/10.1007/s13205-018-1373-1.
54. Ahmad, P., Umar, S., and Sharma, S. (2010). Mechanism of free radical scavenging and role of phytohormones in plants under abiotic stresses. Plant Adapt. Phytoremediation *99*, 99–118. https://doi.org/10.1007/978-90-481-9370-7_5.
55. Wang, W., Zhang, X., Deng, F., Yuan, R., and Shen, F. (2017). Genome-wide characterization and expression analyses of superoxide dismutase (SOD) genes in *Gossypium hirsutum*. BMC Genom. *18*, 376–425. https://doi.org/10.1186/s12864-017-3768-5.
56. Perry, J.J.P., Shin, D.S., Getzoff, E.D., and Tainer, J.A. (2010). The structural biochemistry of the superoxide dismutases. Biochim. Biophys. Acta *1804*, 245–262.

https://doi.org/10.1016/j.bbapap.2009.11.004.
57. Dehury, B., Sarma, K., Sarmah, R., Sahu, J., Sahoo, S., Sahu, M., Sen, P., Modi, M.K., Sharma, G.D., Choudhury, M.D., et al. (2013). In silico analyses of superoxide dismutases (SODs) of rice (*Oryza sativa* L.). J. Plant Biochem. Biotechnol. *22*, 150–156. https://doi.org/10.1007/s13562-012-0121-6.
58. Wang, L., Wang, L., Zhang, Z., Ma, M., Wang, R., Qian, M., and Zhang, S. (2018). Genome-wide identification and comparative analysis of the superoxide dismutase gene family in pear and their functions during fruit ripening. Postharvest Biol. Technol. *143*, 68–77. https://doi.org/10.1016/j.postharvbio.2018.04.012.
59. Zhou, C., Zhu, C., Fu, H., Li, X., Chen, L., Lin, Y., Lai, Z., and Guo, Y. (2019). Genome-wide investigation of superoxide dismutase (SOD) gene family and their regulatory miRNAs reveal the involvement in abiotic stress and hormone response in tea plant (*Camellia sinensis*). PLoS One *14*, e0223609. https://doi.org/10.1371/journal.pone.0223609.
60. Han, L.M., Hua, W.P., Cao, X.Y., Yan, J.A., Chen, C., and Wang, Z.Z. (2020). Genome-wide identification and expression analysis of the superoxide dismutase (SOD) gene family in *Salvia miltiorrhiza*. Gene *742*, 144603. https://doi.org/10.1016/j.gene.2020.144603.
61. Shiu, S.H., and Bleecker, A.B. (2003). Expansion of the receptor-like kinase/Pelle gene family and receptor-like proteins in *Arabidopsis*. Plant Physiol. *132*, 530–543. https://doi.org/10.1104/pp.103.021964.
62. Wang, L., Zhu, W., Fang, L., Sun, X., Su, L., Liang, Z., Wang, N., Londo, J.P., Li, S., and Xin, H. (2014). Genome-wide identification of WRKY family genes and their response to cold stress in *Vitis vinifera*. BMC Plant Biol. *14*, 103–114. https://doi.org/10.1186/1471-2229-14-103.
63. Fink, R.C., and Scandalios, J.G. (2002). Molecular evolution andstructure-function relationships of the superoxide dismutase gene families in angiosperms and their relationship to other eukaryotic and prokaryotic superoxide dismutases. Arch. Biochem. Biophys. *399*, 19–36. https://doi.org/10.1006/abbi.2001.2739.
64. Xu, G., Guo, C., Shan, H., and Kong, H. (2012). Divergence of duplicate genes in exon-intron structure. Proc. Natl. Acad. Sci. USA *109*, 1187–1192. https://doi.org/10.1073/pnas.1109047109.
65. Cao, Y., Li, S., Han, Y., Meng, D., Jiao, C., Abdullah, M., Li, D., Jin, Q., Lin, Y., and Cai, Y. (2018). A new insight into the evolution and functional divergence of FRK genes in *Pyrus bretschneideri*. R. Soc. Open Sci. *5*, 171463. https://doi.org/10.1098/rsos.171463.
66. Yang, X., Tuskan, G.A., and Cheng, M.Z.M. (2006). Divergence of the Dof gene families in poplar, Arabidopsis, and rice suggests multiple modes of gene evolution after duplication. Plant Physiol. *142*, 820–830. https://doi.org/10.1104/pp.106.083642.
67. Ganko, E.W., Meyers, B.C., and Vision, T.J. (2007). Divergence in expression between duplicated genes in *Arabidopsis*. Mol. Biol. Evol. *24*, 2298–2309. https://doi.org/10.1093/molbev/msm158.
68. Buljan, M., and Bateman, A. (2009). The evolution of protein domain families. Biochem. Soc. Trans. *37*, 751–755. https://doi.org/10.1042/BST0370751.
69. Freeling, M. (2009). Bias in plant gene content following different sorts of duplication: tandem, whole-genome, segmental, or by transposition. Annu. Rev. Plant Biol. *60*, 433–453. https://doi.org/10.1146/annurev.arplant.043008.092122.
70. Kersting, A.R., Bornberg-Bauer, E., Moore, A.D., and Grath, S. (2012). Dynamics and adaptive benefits of protein domain emergence and arrangements during plant genome evolution. Genome Biol. Evol. *4*, 316–329. https://doi.org/10.1093/gbe/evs004.
71. Zhong, Y., Jia, Y., Gao, Y., Tian, D., Yang, S., and Zhang, X. (2013). Functional requirements driving the gene duplication in 12 Drosophila species. BMC Genom. *14*, 555–612. https://doi.org/10.1186/1471-2164-14-555.
72. Maruyama-Nakashita, A., Nakamura, Y., Watanabe-Takahashi, A., Inoue, E., Yamaya, T., and Takahashi, H. (2005). Identification of a novel cis-acting element conferring sulfur deficiency response in *Arabidopsis* roots. Plant J. *42*, 305–314. https://doi.org/10.1111/j.1365-313X.2005.02363.x.
73. Osakabe, Y., Yamaguchi-Shinozaki, K., Shinozaki, K., and Tran, L.S.P. (2014). ABA control of plant macroelement membrane transport systems in response to water deficit and high salinity. New Phytol. *202*, 35–49. https://doi.org/10.1111/nph.12613.
74. Samuel Yang, S., Cheung, F., Lee, J.J., Ha, M., Wei, N.E., Sze, S.H., Stelly, D.M., Thaxton, P., Triplett, B., Town, C.D., et al. (2006). Accumulation of genome-specific transcripts, transcription factors and phytohormonal regulators during early stages of fiber cell development in allotetraploid cotton. Plant J. *47*, 761–775. https://doi.org/10.1111/j.1365-313X.2006.02829.x.
75. Patanun, O., Lertpanyasampatha, M., Sojikul, P., Viboonjun, U., and Narangajavana, J. (2013). Computational identification of microRNAs and their targets in cassava (*Manihot esculenta Crantz*.). Mol. Biotechnol. *53*, 257–269. https://doi.org/10.1007/s12033-012-9521-z.
76. Zhang, W., Gao, S., Zhou, X., Chellappan, P., Chen, Z., Zhou, X., Zhang, X., Fromuth, N., Coutino, G., Coffey, M., et al. (2011). Bacteria-responsive microRNAs regulate plant innate immunity by modulating plant hormone networks. Plant Mol. Biol. *75*, 93–105. https://doi.org/10.1007/s11103-010-9710-8.
77. Fernández-Ocaña, A., Chaki, M., Luque, F., Gómez-Rodríguez, M.V., Carreras, A., Valderrama, R., Begara-Morales, J.C., Hernández, L.E., Corpas, F.J., and Barroso, J.B. (2011). Functional analysis of superoxide dismutases (SODs) in sunflower under biotic and abiotic stress conditions. Identification of two new genes of mitochondrial Mn-SOD. J. Plant Physiol. *168*, 1303–1308. https://doi.org/10.1016/j.jplph.2011.01.020.
78. Zhang, W.B., Li, N.N., Qi, F., Chen, X., Hao, J., Yu, C.R., and Lin, X.F. (2014). Isolation and expression analysis of Cu/Zn superoxide dismutase genes from three Caragana species. Russ. J. Plant Physiol. *61*, 656–663. https://doi.org/10.1134/S1021443714050185.
79. Saed-Moucheshi, A., Sohrabi, F., Fasihfar, E., Baniasadi, F., Riasat, M., and Mozafari, A.A. (2021). Superoxide dismutase (SOD) as a selection criterion for triticale grain yield under drought stress: A comprehensive study on genomics and expression profiling, bioinformatics, heritability, and phenotypic variability. BMC Plant Biol. *21*, 148–219. https://doi.org/10.1186/s12870-021-02919-5.
80. Gupta, A.S., Heinen, J.L., Holaday, A.S., Burke, J.J., and Allen, R.D. (1993). Increased resistance to oxidative stress in transgenic plants that overexpress chloroplastic Cu/Zn superoxide dismutase. Proc. Natl. Acad. Sci. USA *90*, 1629–1633. https://doi.org/10.1073/pnas.90.4.162.
81. Diaz-Vivancos, P., Faize, M., Barba-Espin, G., Faize, L., Petri, C., Hernández, J.A., and Burgos, L. (2013). Ectopic expression of cytosolic superoxide dismutase and ascorbate peroxidase leads to salt stress tolerance in transgenic plums. Plant Biotechnol. J. *11*, 976–985. https://doi.org/10.1111/pbi.12090.
82. Del Río, L.A. (2015). ROS and RNS in plant physiology: an overview. J. Exp. Bot. *66*, 2827–2837. https://doi.org/10.1093/jxb/erv099.
83. Mittler, R., Vanderauwera, S., Gollery, M., and Van Breusegem, F. (2004). Reactive oxygen gene network of plants. Trends Plant Sci. *9*, 490–498. https://doi.org/10.1016/j.tplants.2004.08.009.
84. You, J., and Chan, Z. (2015). ROS regulation during abiotic stress responses in crop plants. Front. Plant Sci. *6*, 1092. https://doi.org/10.3389/fpls.2015.01092.
85. Wu, J., Zhang, J., Li, X., Xu, J., and Wang, L. (2016). Identification and characterization of a PutCu/Zn-SOD gene from *Puccinellia tenuiflora* (Turcz.) Scribn. et Merr. Plant Growth Regul. *79*, 55–64. https://doi.org/10.1007/s10725-015-0110-6.
86. Li, Z., Zhang, H., Ge, S., Gu, X., Gao, G., and Luo, J. (2009). Expression pattern divergence of duplicated genes in rice. BMC Bioinf. *10*, S8. https://doi.org/10.1186/1471-2105-10-S6-S8.
87. Boher, B., and Verdier, V. (1994). Cassava bacterial blight in Africa: the state of knowledge and implications for designing control strategies *2*, 505–509.
88. Lopez, C., Soto, M., Restrepo, S., Piégu, B., Cooke, R., Delseny, M., Tohme, J., and Verdier, V. (2005). Gene expression profile in response to *Xanthomonas axonopodis pv. manihotis* infection in cassava using a cDNA microarray. Plant Mol. Biol. *57*, 393–410. https://doi.org/10.1007/s11103-004-7819-3.
89. Wydra, K., Banito, A., and Kpémoua, K.E. (2007). Characterization of resistance of cassava genotypes to bacterial blight by evaluation of leaf and systemic symptoms in relation to yield in different ecozones. Euphytica *155*, 337–348. https://doi.org/10.1007/s10681-006-9335-9.
90. Bart, R., Cohn, M., Kassen, A., McCallum, E.J., Shybut, M., Petriello, A., Krasileva, K., Dahlbeck, D., Medina, C., Alicai, T., et al. (2012). High-throughput genomic sequencing of cassava bacterial blight strains identifies conserved effectors to target for durable resistance. Proc. Natl. Acad. Sci. USA *109*, E1972–E1979. https://doi.org/10.1073/pnas.1208003109.
91. Muñoz-Bodnar, A., Perez-Quintero, A.L., Gomez-Cano, F., Gil, J., Michelmore, R., Bernal, A., Szurek, B., and Lopez, C. (2014). RNAseq analysis of cassava reveals similar plant responses upon infection with pathogenic and non-pathogenic strains of

Xanthomonas axonopodis pv. manihotis. Plant Cell Rep. 33, 1901–1912. https://doi.org/10.1007/s00299-014-1667-7.

92. Wei, Y., Chang, Y., Zeng, H., Liu, G., He, C., and Shi, H. (2018). RAV transcription factors are essential for disease resistance against cassava bacterial blight via activation of melatonin biosynthesis genes. J. Pineal Res. 64, e12454. https://doi.org/10.1111/jpi.12454.
93. Li, X., Fan, S., Hu, W., Liu, G., Wei, Y., He, C., and Shi, H. (2017). Two cassava basic leucine zipper (bZIP) transcription factors (MebZIP3 and MebZIP5) confer disease resistance against cassava bacterial blight. Front. Plant Sci. 8, 2110. https://doi.org/10.3389/fpls.2017.02110.
94. Tuo, D., Zhou, P., Yan, P., Cui, H., Liu, Y., Wang, H., Yang, X., Liao, W., Sun, D., Li, X., et al. (2021). A cassava common mosaic virus vector for virus-induced gene silencing in cassava. Plant Method 17, 74. https://doi.org/10.1186/s13007-021-00775-w.
95. Pflieger, S.P., Richard, M.M.S., Blanchet, S., Meziadi, C., and Geffroy, V.R. (2013). VIGS technology: an attractive tool for functional genomics studies in legumes. Funct. Plant Biol. 40, 1234–1248. https://doi.org/10.1071/FP13089.
96. Wei, Y., Liu, G., Bai, Y., Xia, F., He, C., Shi, H., and Foyer, C. (2017). Two transcriptional activators of N-acetylserotonin O-methyltransferase 2 and melatonin biosynthesis in cassava. J. Exp. Bot. 68, 4997–5006. https://doi.org/10.1093/jxb/erx305.
97. Chen, C., Chen, H., Zhang, Y., Thomas, H.R., Frank, M.H., He, Y., and Xia, R. (2020). TBtools: an integrative toolkit developed for interactive analyses of big biological data. Mol. Plant 13, 1194–1202. https://doi.org/10.1016/j.molp.2020.06.009.
98. Gasteiger, E., Hoogland, C., Gattiker, A., Wilkins, M.R., Appel, R.D., and Bairoch, A. (2005). Protein identification and analysis tools on the ExPASy server. Proteomics Protoc. Handbook, 571–607. https://doi.org/10.1385/1-59259-890-0:5710.
99. Yuan, J., Amend, A., Borkowski, J., DeMarco, R., Bailey, W., Liu, Y., Xie, G., and Blevins, R. (1999). MULTICLUSTAL: a systematic method for surveying Clustal W alignment parameters. Bioinformatics 15, 862–863. https://doi.org/10.1093/bioinformatics/15.10.862.
100. Bailey, T.L., Johnson, J., Grant, C.E., and Noble, W.S. (2015). The MEME suite. Nucleic Acids Res. 43, W39–W49. https://doi.org/10.1093/nar/gkv416.
101. Hu, B., Jin, J., Guo, A.-Y., Zhang, H., Luo, J., and Gao, G. (2015). GSDS 2.0: an upgraded gene feature visualization server. Bioinformatics 31, 1296–1297. https://doi.org/10.1093/bioinformatics/btu817.
102. Wang, Y., Tang, H., DeBarry, J.D., Tan, X., Li, J., Wang, X., Lee, T.-H., Jin, H., Marler, B., Guo, H., et al. (2012). MCScanX: a toolkit for detection and evolutionary analysis of gene synteny and collinearity. Nucleic Acids Res. 40, e49. https://doi.org/10.1093/nar/gkr1293.
103. Kayum, M.A., Park, J.-I., Nath, U.K., Saha, G., Biswas, M.K., Kim, H.-T., and Nou, I.S. (2017). Genome-wide characterization and expression profiling of PDI family gene reveals function as abiotic and biotic stress tolerance in Chinese cabbage (Brassica rapa ssp. pekinensis). BMC Genom. 18, 885–920. https://doi.org/10.1186/s12864-017-4277-2.
104. Khaja, R., MacDonald, J.R., Zhang, J., and Scherer, S.W. (2006). Methods for identifying and mapping recent segmental and gene duplications in eukaryotic genomes. Methods Mol. Biol. 338, 9–20. https://doi.org/10.1385/1-59745-097-9:9.
105. Gu, Z., Cavalcanti, A., Chen, F.C., Bouman, P., and Li, W.H. (2002). Extent of gene duplication in the genomes of Drosophila, nematode, and yeast. Mol. Biol. Evol. 19, 256–262. https://doi.org/10.1093/oxfordjournals.molbev.a004079.
106. Lescot, M., Déhais, P., Thijs, G., Marchal, K., Moreau, Y., Van de Peer, Y., Rouzé, P., and Rombauts, S. (2002). PlantCARE, a database of plant cis-acting regulatory elements and a portal to tools for in silico analysis of promoter sequences. Nucleic Acids Res. 30, 325–327.
107. Griffiths-Jones, S., Grocock, R.J., Van Dongen, S., Bateman, A., and Enright, A.J. (2006). miRBase: microRNA sequences, targets and gene nomenclature. Nucleic Acids Res. 34, D140–D144. https://doi.org/10.1093/nar/gkj112.
108. Franceschini, A., Szklarczyk, D., Frankild, S., Kuhn, M., Simonovic, M., Roth, A., Lin, J., Minguez, P., Bork, P., Von Mering, C., and Jensen, L.J. (2013). STRING v9. 1: protein-protein interaction networks, with increased coverage and integration. Nucleic Acids Res. 41, D808–D815. https://doi.org/10.1093/nar/gks1094.
109. Livak, K.J., and Schmittgen, T.D. (2001). Analysis of relative gene expression data using real-time quantitative PCR and the $2^{-\Delta\Delta CT}$ method. Methods 25, 402–408. https://doi.org/10.1006/meth.2001.1262.
110. Schmittgen, T.D., and Livak, K.J. (2008). Analyzing real-time PCR data by the comparative CT method. Nat. Protoc. 3, 1101–1108. https://doi.org/10.1038/nprot.2008.73.

STAR★METHODS

KEY RESOURCES TABLE

REAGENT or RESOURCE	SOURCE	IDENTIFIER
Bacterial and virus strains		
Xanthomonas phaseoli pv. *manihotis* (*Xpm*) strain (CHN11)	Stored in our lab	N/A
DH5α--competent cell	WEIDI	DL1001S; CAT#: DL1001
GV3101 (pSoup-p19)–competent cell	WEIDI	AC1003S; CAT#: AC1003
Biological samples		
Healthy cassava leaves	Chen Yinhua Laoboratory	N/A
Chemicals, peptides, and recombinant proteins		
RNAprep Pure Plant Plus Kit (Polysaccharides & Polyphenolics-rich)	TIANGEN	DP441
reverse transcriptase kit	TIANGEN	KR118-02
TB Green Premix Ex Taq II	TAKARA	RR820B
PrimeSTAR	TAKARA	R045A
Nimble cloning kit	NC Biotech	NC001
Deposited data		
transcriptome data after infected by *Xpm*668	This paper	GEO: PRJNA257332
transcriptome data in various SC8 tissues	This paper	GEO: PRJNA324539, GSE82279
Experimental models: Organisms/strains		
cassava cultivar South China 8 (*Manihot esculenta* Crantz, SC8)	National Cassava Germplasm Nursery (Danzhou, China)	SC8
Oligonucleotides		
Primers for detecting the expression of *MeSODs*, see Table S11	This paper	N/A
Recombinant DNA		
Plasmid: pCsCMV-*MeMSOD2*	This paper	N/A
Plasmid: pCsCMV-*ChI*	This paper	N/A
Software and algorithms		
TBtools	Chen et al.[97]	https://github.com/CJ-Chen/TBtools/releases; RRID: SCR_023018
ImageJ	Schneider et al.[53]	https://ImageJ.nih.gov/ij/; RRID: SCR_003070

RESOURCE AVAILABILITY

Lead contact

Further information and requests for resources and reagents should be directed to and will be fulfilled by the lead contact, Yinhua Chen, yhchen@hainanu.edu.cn.

Material availability

This study did not generate new unique reagents.

Data and code availability

- Transcriptome data after *Xpm668* inoculation have been deposited at GEO and are publicly available as of the publication date. Accession numbers are listed in the key resources table. All data reported in this paper will be shared by the lead contact upon request.

- This paper does not report original code.
- Any additional information required to reanalyze the data reported in this paper is available from the lead contact upon request.

EXPERIMENTAL MODEL AND STUDY PARTICIPANT DETAILS

The cassava cultivar South China 8 (*Manihot esculenta* Crantz, SC8) was utilised in this study and obtained from the National Cassava Germplasm Nursery (Danzhou, China). Approximate 15-cm stems containing two to three buds were grown in a glasshouse at 35/20°C (day/night temperatures) under a 12/8-h photoperiod and 80% relative humidity from April to July 2020. All stems were grown in plastic pots (soil: vermiculite = 1:1; height × upper diameter × bottom diameter = 18.8 × 18.5 × 14.8 cm) (Fu et al., 2016). Twenty days later, plants at similar growth stages were selected and subjected to stress treatments. Fresh leaves were harvested and immediately frozen in liquid nitrogen, then stored at −80°C until use. The experiments were conducted at least twice.

To investigate the expression profile of *MeSOD* genes in response to salt stress, cassava seedlings were treated with a 300 mM NaCl solution. Subsequently, the third and fifth leaves from the top were collected at 1, 3, 6, and 24 h.

For drought, cassava seedlings were treated with polyethylene glycol (PEG) 6000 solution (30% concentration) as the treatment group and tap water as the control. The roots, stems, and leaves were collected after 2, 6, 12, 24, and 48 h.

For cassava bacterial blight (CBB) infection, the *Xanthomonas phaseoli* pv. *manihotis* (*Xpm*) strain (CHN11) was used. The inoculation followed the method described with minor modifications (Lopez et al., 2005). Five plants were inoculated with *Xpm*CHN11 by dropping 10-μL bacterial suspension of 1 × 108 CFU/mL [optical density at 600 nm (OD_{600}) = 0.1] into a 2-mm-diameter hole. The third and fifth leaves from the top were inoculated using a sterile syringe. Cassava seedlings were sampled at 3 and 6 h, 1-, 3-, and 6-days post-inoculation. qRT-PCR was used to determine the expression profile of *MeSOD* genes of collected tissues following salinity, PEG, and CBB treatments.

METHOD DETAILS

Identification and sequence analyses of SOD gene family in cassava

Cassava genomic, protein, and coding sequences were downloaded from the Phytozome database (https://phytozome-next.jgi.doe.gov/). The protein sequences of 9 *Oryza sativa* SODs (*OsSODs*) and 7 *A. thaliana* SODs (*AtSODs*) were used as queries to identify all potential SOD protein sequences in cassava using a BLASTp search E-value threshold of 1.0×10^{-5}. The obtained candidate sequences were considered SODs for *M. esculenta*. Multiple sequence alignment of candidate sequences was performed by DNAMAN 7 software. Furthermore, the Pfam, conserved domain databases (CDD) and SMART website were used to determine the presence of the SOD domains: Cu-ZnSOD (PF00080) and Fe-MnSOD (PF02777 and PF00081). The prefix 'Me' was used to denote cassava, followed by CSOD for Cu-Zn*SOD*, FSOD for Fe-SOD, and MSOD for Mn-SOD. The following Arabic numerals indicate cassava SOD genes with the same domain, and the numerical order is determined according to the position of the genes on the chromosome. The physicochemical characteristics of MeSOD proteins were predicted using the ProtParam tool (http://web.expasy.org/protparam/), and the parameters, including the molecular weight (MW), theoretical isoelectric point (pI), and grand average of hydropathicity index (GRAVY) were determined.[98] The subcellular localization of the identified protein was predicted using WoLF PSORT (https://wolfpsort.hgc.jp/).

Phylogenetic relationship, conserved motif, and gene structure analysis

To study the evolutionary relationship between *MeSODs* and those from other species, a total of 47 protein sequences, including 8 *MeSODs*, 7 AtSODs, 6 *D. longan* (DlSODs), 9 OsSODs, 13 *M. acuminata* (MaSODs) and 4 *Populus trichocarpa* (PtSODs), were aligned using ClustalW programme with the default parameters.[99] MEGA7.1 software was employed to construct an unrooted phylogenetic tree using the neighbor-joining (NJ) phylogenetic method with 1000 bootstrap replicates.

Multiple Expectation Maximization for Motif Elicitation (MEME, version 4.9.1.) suite (http://meme-suite.org/tools/meme) was used to predict the conserved motif of the *MeSOD* gene sequences.[100] The relative parameters were set to an optimum motif width of 6–50 and a maximum of 10 motifs. The Gene Structure Display Server GSDS (version 2.0, http://gsds.cbi.pku.edu.cn/index.php) was used to analyse the *MeSOD* gene structures.[101] The *MeSOD* gene structures and conserved motif results were displayed with TBtools software.[97] The secondary and tertiary structures of *MeSOD* genes were modelled using SWISS MODEL server (https://swissmodel.expasy.org/).

Chromosomal location, whole-genome duplication, and synteny analysis

The cassava genomic annotation file GFF (General Feature Format) was retrieved from the Phytozome database (https://phytozome-next.jgi.doe.gov/), following the extraction of the annotation of *MeSOD* gene. The chromosomal location of *MeSOD* genes was determined using the GFF files. The chromosomal distribution of *MeSOD* genes was visualised using the TBtools programme[97] The syntenic relationship was analysed using the Multiple Collinearity Scan (MCScanX) Toolkit.[102] The duplicated *MeSOD* genes are classified as whole-genome duplications (WGDs). Tandem duplicated genes were defined as two or more homologous genes separated by 100 kb on a single chromosome with no intervening gene.[103] Nucleotide blast (BLASTN) was used to detect segmental duplicate genes (score < $1e^{-5}$), flanking 100 kb of coding sequence (CDS; both 50 kb upstream and downstream). The duplicate genes were further confirmed following the criteria: (i) sequence alignment length > 200 bp, and (ii) sequence identity > 85%.[104,105] To explore the mechanism of gene divergence after duplication, the number of substitutions per non-synonymous (Ka) and synonymous (Ks) was calculated using TBtools under the default parameters.[97]

Regulatory elements analysis of *MeSOD* genes and prediction of miRNA targets

To demonstrate the possible regulatory mechanism of SOD genes in environmental stress responses under natural conditions, the PlantCARE database (http://bioinformatics.psb.ugent.be/webtools/plantcare/html/) was used to identify *cis*-acting regulatory elements of *MeSOD* genes in the 2.0 kb of the 5′ regulatory regions from translational start sites.[106] The data were visualized with the TBtools programme. The cassava miRNA sequences were obtained from miRBase (http://www.mirbase.org/).[107] The putative target sites of miRNA candidates were predicted with the plant small RNA Target analysis (psRNATarget) server with default parameters (http://plantgrn.noble.org/psRNATarget/?function=3) by aligning the miRNA sequences with 5′ and 3′ Untranslated Regions (UTRs) and the CDS of all *MeSOD* genes.[107]

Protein-protein interaction (PPI) network of MeSOD genes

Arabidopsis interologues were used to predict the PPI network and examine the *MeSOD* protein's relationship. The functional protein association network was analysed using the STRING database (https://cn.string-db.org/) with a confidence score of 0.15. The PPI network was inferred with the default parameter.[108]

GO annotation and tissue-specific expression profile of MeSOD genes

The GO terms of the *MeSOD* genes were extracted from the NCBI database (https://www.ncbi.nlm.nih.gov/). The GO enrichment analysis was conducted using omicshare tool (https://www.omicshare.com/tools/Home/Soft/gogsea). The biological processes, cellular localisation, and molecular functions of the 8 *MeSOD* proteins were investigated. The transcriptome data were retrieved from the NCBI database (accession numbers: PRJNA324539, and GEO Dataset: GSE82279) and used to investigate the expression profiles of *MeSOD* genes, after being infected with *Xpm*CHN11, in various SC8 tissues (Wilson et al., 2016). The latter include the tissue from the leaves, midveins, lateral buds, somatic embryos (OES), brittle calluses (FEC), fibrous roots (FR), root tubers (SR), stems, petioles, root tips (RAM), and stem apexes (SAM). Reads per kilobase per million mapped reads (RPKM) values were calculated to evaluate the gene expression.

Expression pattern profiling of MeSODs under various abiotic stresses

Transcriptome data for cold stress and drought stress were obtained from the NCBI database. The RPKM values were calculated following the method previously described.[98] Subsequently, heat maps of the expression patterns were generated using TBtools.[97]

Construction of VIGS vector of *MeMSOD2* and infection of 'SC8' cassava

The online software SGN VIGS Tool (https://vigs.solgenomics.net/) was utilized to design the silencing target gene induced by *MeMSOD2*, and the recombinant plasmid pCsCMV-MeMSOD2 was constructed using the Nimble cloning kit. The recombinant plasmid was then transferred to Agrobacterium GV3101, and a positive monoclonal clone was selected and cultured in an LB liquid medium containing kanamycin and rifampicin (50 mg/L and 25mg/L, respectively) overnight. Subsequently, the bacteria were collected at 4000 rpm and washed three times with 10 mmol/L MgCl2. The suspension was then enhanced using 1 mol/L MES, 1 mol/L MgCl2, and 200 mmol/L AS (acetosyringone), and the OD_{600} was adjusted to 1. The recombinant plasmid containing the whole sequence of the CsCMV virus and the silencing target gene *ChlI* (pCsCMV-ChlI) were used as the negative and positive controls, respectively. Each treatment group had three biological replicates, and three healthy leaves were selected for each plant. The suspended bacterial solution was injected into both sides of the main vein on the back of each cassava leaf using a 1 mL syringe. Each leaf was inoculated on ten spots, with approximately 10μL injected into each hole. After 30 days of infection, the positive control leaves showed an albino chlorosis phenotype. The total RNA of cassava new leaves in both the negative control and experimental groups was extracted and reverse-transcribed into cDNA to detect the target gene expression level.

QUANTIFICATION AND STATISTICAL ANALYSIS

Total RNA was isolated with the RNAprep Pure Plant Plus Kit [(Polysaccharides & Polyphenolics-rich) (DP441, TIANGEN, Beijing, China)] following the manufacturer's instructions. RNA concentration determination, DNase I (1 U/μL) treatment, cDNA synthesis, qRT-PCR, and data analysis were performed following a published protocol with minor modifications,[109,110] and $P < 0.05$ was defined as significant in the drawing of the bar chart. The first cDNA strand was synthesised using a reverse transcriptase kit (M1631, Thermo, USA). The gene-specific primers (Table S11) were designed with the NCBI Primer-BLAST tool (https://www.ncbi.nlm.nih.gov/tools/primer-blast/index.cgi?LINK_LOC=BlastHome). Real-time PCR was performed using a 7500 Real-Time PCR System (Applied Biosystems) with a total reaction volume of 20 μL consisting of 2 μL cDNA, 1 μL 10 μM forward primer, 1 μL 10 μM reverse primer, 10 μL qRT-PCR Master Mix, and 6 μL sterilised ddH_2O. The real-time PCR amplification conditions were set as follows: denaturation at 95°C for 30 s, followed by 40 cycles of 95°C for 5 s, 55°C for 30 s, 72°C for 30 s, and 72°C for 10 min. The EF1α gene (accession number: Manes.15G054700) was selected to calculate the relative fold differences using the $2^{-\Delta\Delta CT}$ method [$\Delta\Delta C_T = (Ct_{\text{target gene}} - Ct_{EF1\alpha})$].[110] Three sets of biological replicates and three sets of technical replicates were analyzed. All of the statistical details of the experiments can be found in the results section.